geosciences

MDPI

Article

Stratigraphic and Tectonic Setting of the Liguride Units Cropping Out along the Southeastern Side of the Agri Valley (Southern Apennines, Italy)

Giacomo Prosser [1], Giuseppe Palladino [2,3,*], Dario Avagliano [4], Francesco Coraggio [4], Eleonora Maria Bolla [5], Marcello Riva [5] and Daniele Enrico Catellani [5]

1 Dipartimento di Scienze, Università degli Studi della Basilicata, 85100 Potenza, Italy; giacomo.prosser@unibas.it
2 Department of Geology and Geophysics, School of Geosciences, University of Aberdeen, Aberdeen AB24 3UF, UK
3 Italconsult S.p.A., Viggiano, 85059 Potenza, Italy
4 ENI S.p.A., Viggiano, 85059 Potenza, Italy; dario.avagliano@eni.com (D.A.); francesco.coraggio@eni.com (F.C.)
5 ENI S.p.A., San Donato Milanese, 20097 Milano, Italy; eleonora.maria.bolla@eni.com (E.M.B.); marcello.riva@eni.com (M.R.); daniele.enrico.catellani@eni.com (D.E.C.)
* Correspondence: giuseppe.palladino@abdn.ac.uk

check for updates

Citation: Prosser, G.; Palladino, G.; Avagliano, D.; Coraggio, F.; Bolla, E.M.; Riva, M.; Catellani, D.E. Stratigraphic and Tectonic Setting of the Liguride Units Cropping Out along the Southeastern Side of the Agri Valley (Southern Apennines, Italy). *Geosciences* **2021**, *11*, 125. https://doi.org/10.3390/geosciences11030125

Academic Editors: Domenico Liotta, Giancarlo Molli and Jesus Martinez-Frias

Received: 30 December 2020
Accepted: 4 March 2021
Published: 9 March 2021

Publisher's Note: MDPI stays neutral with regard to jurisdictional claims in published maps and institutional affiliations.

Copyright: © 2021 by the authors. Licensee MDPI, Basel, Switzerland. This article is an open access article distributed under the terms and conditions of the Creative Commons Attribution (CC BY) license (https://creativecommons.org/licenses/by/4.0/).

Abstract: This paper shows the main results of a multidisciplinary study performed along the southeastern sector of the Agri Valley in Basilicata (Southern Italy), where Cenozoic units, crucial for constraining the progressive evolution of the Southern Apennine thrust and fold belt and, more in general, the geodynamic evolution of the Mediterranean area are widely exposed. In particular, we aimed at understanding the stratigraphic and tectonic setting of deep-sea, thrust-top Cenozoic units exposed immediately to north of Montemurro, between Costa Molina and Monte dell'Agresto. In the previous works different units, showing similar sedimentological characteristics but uncertain age attribution, have been reported in the study area. In our study, we focussed on the Albidona Formation, pertaining to the Liguride realm, which shows most significant uncertainties regarding the age and the stratigraphic setting. The study was based on a detailed field survey which led to a new geological map of the area. This was supported by new stratigraphic, biostratigraphic and structural analyses. Biostratigraphic analysis provided an age not older than the upper Ypresian and not younger than the early Priabonian. Recognition of marker stratigraphic horizons strongly helped in the understanding of the stratigraphy of the area. The study allowed a complete revision of the stratigraphy of the outcropping Cenozoic units, the recognition of until now unknown tectonic structures and the correlation between surface and subsurface geology.

Keywords: Albidona Formation; biostratigraphy; liguride units; Agri Valley; southern Apennines

1. Introduction

Understanding surface geology of a given area provides fundamental clues on the lithological, stratigraphic and structural setting of the subsurface, useful for exploitation of natural resources. In particular, recognition of key stratigraphic horizons is essential for the correct identification of major tectonic structures and the interpretation and correlation of geophysical and well data to define reliable 3D geological models. In addition, the recognition of regional faults and permeable stratigraphic units can be helpful in modelling fluid flow in subsurface. The Agri Valley represents a good example where a better definition of the surface geology provides significant improvements in the interpretation of subsurface data.

Here, the carbonate reservoir rocks are covered by a thick pile of allochthonous thrust sheets emplaced during the building of the southern Apennine thrust and fold belt (Figure 1).

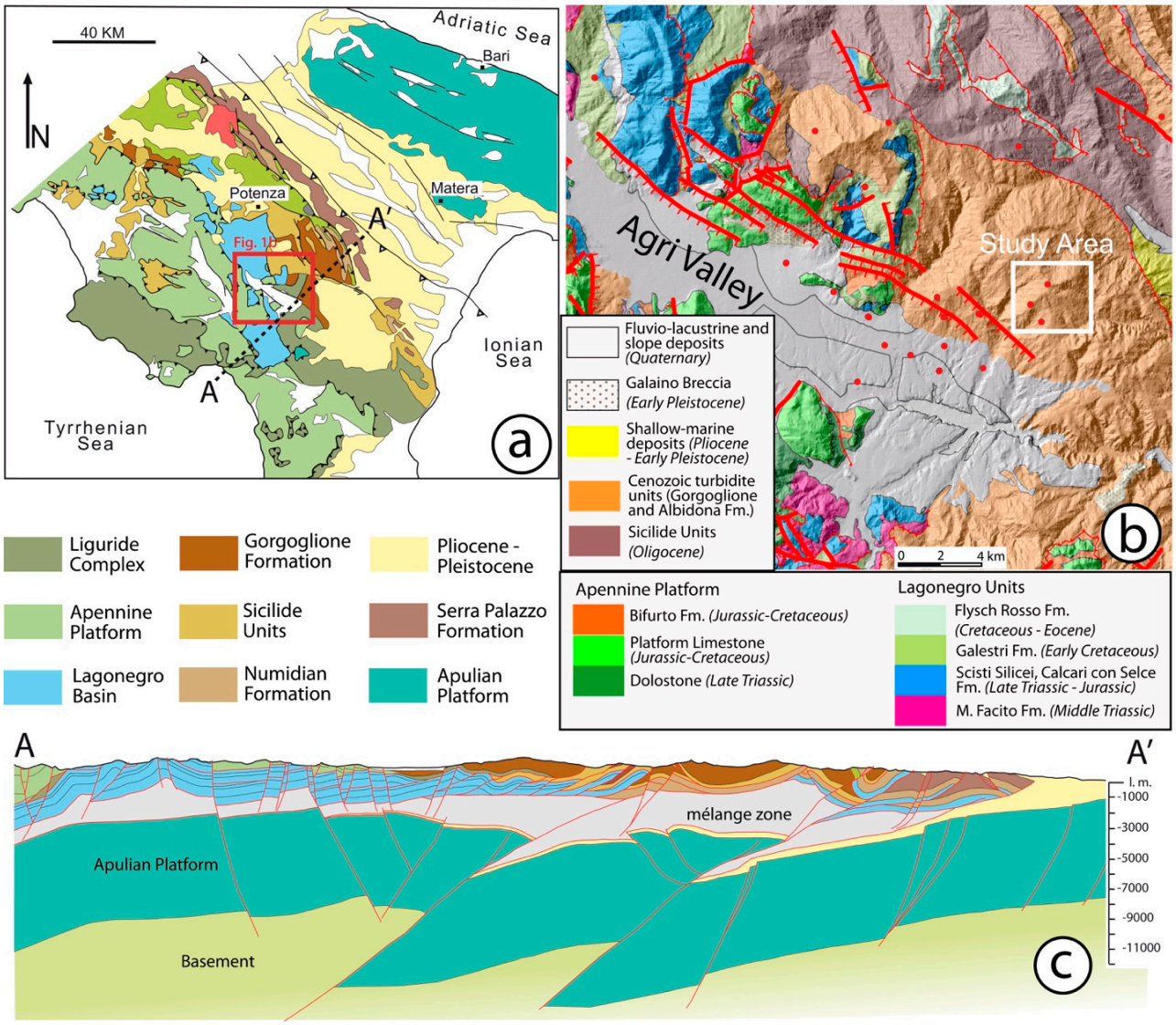

Figure 1. (**a**) Regional geological map of the Southern Apennines; (**b**) schematic sketch map of the Agri Valley graben showing the location of the study area; (**c**) schematic geological cross-section outlining the structural highs of the Internal Apulian Platform and the geometry of the overlying allochthonous units [1].

For this reason, the knowledge of the surface geology in this area is regarded as a priority. In the Agri Valley one of the major geological challenges consists in the distinction between different Cenozoic turbidite units, represented by the Albidona and the Gorgoglione formations sensu [2] and named "Albidona Formation" and "Gorgoglione Flysch" in the Italian Geological Map at 1:50,000 scale (CARG Project—e.g., Servizio Geologico d'Italia, 2005, 2009, 2014). The latter units are commonly interpreted as part of allochthonous thrust sheets. According to [3] the aforementioned formations commonly show similar lithological and sedimentological characteristics, which frequently hinder the correct identification of the vertical/lateral relationships. These issues, along with the scarce paleontological age determinations, led to stratigraphic misinterpretations and failure in recognizing important tectonic structures in the field that are fundamental when building a 3D geological model of the Agri Valley. Difficulty in discriminating between the

Albidona and the Gorgoglione formations is evident when comparing different geological maps of the Agri Valley area [3–6].

Although the Albidona and the Gorgoglione formations show similar lithological characteristics (in both the cases these formations consist of alternating turbiditic sandstone/conglomerates and clays) their correct attribution has significant geological, hydrogeological and environmental consequences. In addition, the correct mapping and the detailed definition of the boundaries (stratigraphic or tectonic) between the two aforementioned formations and a more precise definition of their age is also helpful for providing information on the evolution of the southern Apennine thrust and fold belt.

In this paper we show the main results of detailed geological mapping, accompanied by new stratigraphic and structural reconstructions, carried out in the Costa Molina—Tempa del Vento—La Rossa—Monte dell'Agresto area, located in the southeastern sector of the Agri Valley (Figure 2a,b). The study has been supported by new biostratigraphic data, performed on marker stratigraphic horizons, that have been used to precisely discriminate the Albidona and Gorgoglione formations. In addition, the new stratigraphic data provided evidence for important tectonic structures that have been recognized for the first time in the area.

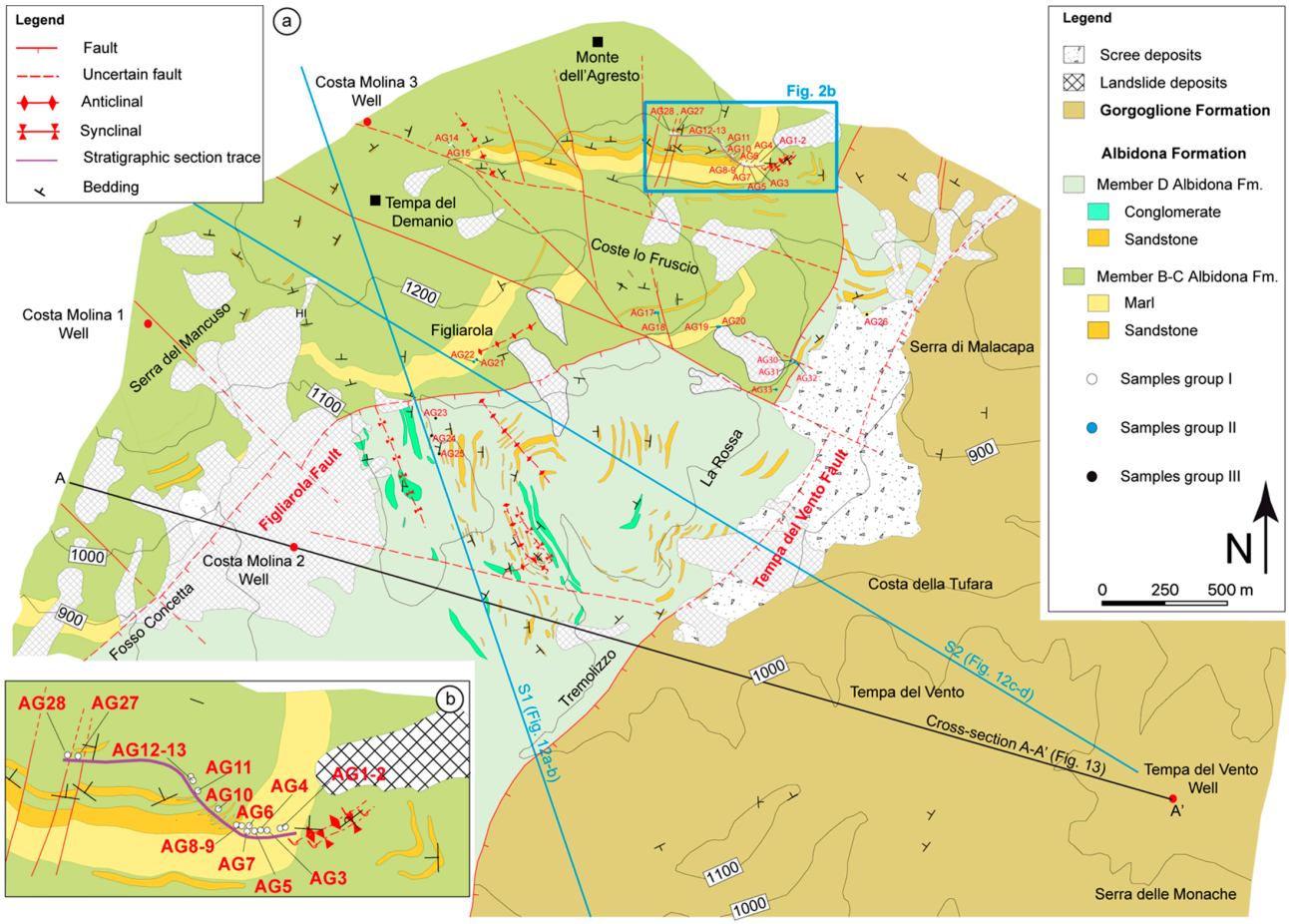

Figure 2. (**a**) Geological map of the Costa Molina—Monte dell'Agresto-Tempa del Vento area, showing (**b**) the location of the studied stratigraphic section, collected samples, seismic lines and geological cross section.

2. Geological Setting

The Agri Valley is a Quaternary tectonic depression, filled up with continental deposits, located in the axial sector of the southern Apennine thrust belt [7,8]. Its origin is mainly connected to the activity of Pliocene to Quaternary, NW-SE oriented, strike-slip and normal faults, which started to develop when thrusting was still active in the frontal sector of the belt [9,10]. In particular, in the southern Apennines extensional tectonics strictly reflects the eastward roll-back and crustal delamination of the of the Apulian slab, associated with the Tyrrhenian backarc basin opening [11–14]. Based on the available field and subsurface data, the Agri Valley is considered a Quaternary graben [15] controlled by two major bounding faults named, respectively, Eastern Agri Fault System (EAFS) and Monti della Maddalena fault system (MMFS) [16]. Active tectonics in the area is testified by recent continental deposits displaced by normal faults [7] and by the intense seismicity currently characterizing the Agri Valley area [17,18].

The Agri Valley graben developed on a pre-Pliocene substratum formed by a series of stacked allochthonous units forming the axial sector of the southern Apennine thrust belt. In the study sector, the architecture of the mountain belt can be observed on outcrops in the shoulders of the Agri Valley graben, or reconstructed by means of the abundant subsurface data (seismic lines and wells) acquired for hydrocarbon exploration [19]. The geometrically highest allochthonous unit is represented by the Liguride complex, consisting of minor fragments of oceanic crust, pertaining to Ligurian part of the Alpine Tethys realm [20], and the related sedimentary cover of Mesozoic to Cenozoic age [4]. This complex derives from a late Cretaceous–early Miocene accretionary wedge, formed on top of the NW-dipping subduction of the Ligurian Tethys [21,22]. All the underlying tectonic units pertain to the paleomargin of the African plate and are represented by the Apennine Platform carbonates, tectonically superimposed onto the deep-water deposits of the Lagonegro Basin, and the Apulian Platform carbonates that represent the lowest structural element of the southern Apennine tectonic pile. Emplacement of the allochthonous units took place during the middle to late Miocene and was accommodated by major low-angle thrusts, bounding at the base each tectonic unit [23,24]. However, severe internal deformation can be also recognized, as testified by folding, thrusting and local development of cleavage fabrics within the clay-rich intervals. This deformation style particularly well outlined in the Lagonegro Units, locally consisting of thick antiformal stacks, as documented by hydrocarbon well data [2]. The simple piling relationship between individual allochthonous units is frequently made more complex by out of sequence thrusting processes, produced during the latest deformation events of late Pliocene-early Pleistocene age [25,26].

The northeastward propagation of thrusting during formation of the Southern Apennines is recorded by a series of thrust-sheet top basins that rejuvenate progressively toward NE, according to the emplacement age of the allochthonous units. Typical thrust-sheet top deposits in the Agri Valley area, as indicated by previous literature [3], are represented by the Albidona and Gorgoglione formations. In particular, in the study area (Figure 2a) the Albidona Formation is stratigraphically covered by the Gorgoglione Formation by means a marked angular unconformity [2]. The latter formation has been deposited in two major NW-trending sub-basins, whose location and evolution were controlled by thrusting and folding within the underlying allochthonous units [27]. The study area corresponds to the western sub-basin, where the Gorgoglione Formation appears less involved by later thrusting and consequent tectonic load with respect to the eastern sub-basin [28,29]. According to the literature [30], the basal unconformity of the Gorgoglione Formation on the Albidona Formation has been intercepted by hydrocarbon wells drilled in the study area (i.e., the Costa Molina2 well). However, the same contact is less recognizable in the field because of striking lithological similarities between the Gorgoglione and Albidona formations. Although few doubts exist about the stratigraphic relationships between the two considered units, different interpretations still persist about the age and the significance of the Albidona Formation. The chronostratigraphic attribution of

the Albidona Formation, the problems in discriminating it from the Gorgoglione Formation and the related tectonic and geodynamic implications will be discussed in the following section.

3. The Age and Significance of the Albidona Formation

The Albidona Formation mainly consists of siliciclastic turbidite, outlined by sandstone and conglomerate beds, alternating with intervals of shales, marls and silty marls, with a thickness of about 2000 m in the type locality of Albidona in Northern Calabria [31–33]. A typical feature is represented by the occurrence of about 50 m thick intervals of nearly homogeneous whitish marly limestones and marls, particularly frequent in the lower-intermediate part of the succession. The presence of both siciliclastic and calciclastic intervals suggests that sediments were supplied both from an active margin undergoing contractional deformation and from the marginal part of a carbonate platform [34]. According to Colella and Zuffa [35], the siliciclastic material as well as olistoliths of ophiolitic rocks [36] were fed by the Liguride accretionary wedge, located to the west, whereas the carbonate debris was supplied by the western marginal portion of the Apennine Platform, located to the east. Accordingly, the thick marly intervals were interpreted as carbonate turbidite megabeds [35]. The same intervals have been compared by Baruffini et al. ii [33] to the "homogenites" recognized in the deep-sea Holocene successions of the Mediterranean Sea [37], interpreted as tsunami-derived megaturbidites [38].

The age of the Albidona Formation is controversial. Selli [31], who described for the first time the formation, provided a Langhian age. On the other hand, several authors [39–44] obtained older Eocene ages by analysing planktonic foraminifera both in the type locality and in other sections of the southern Apennines. However, similar studies on the Albidona type section allowed to obtain Oligocene-early Burdigalian ages [32]. Younger ages (early–middle Burdigalian) were provided by Bonardi et al. ii [45] from the analysis of nannofossils in five samples collected in the type locality and in the Agri Valley. Based on a detailed analysis of calcareous nannofossils and palynomorphs from the Albidona type section, Baruffini et al. ii [33] reported again Eocene ages, similar to those already documented in the older studies and discussed also the Miocene ages indicated by the previous authors. In particular, they provided an early Ypresian to early Priabonian age and recognized a wide *hiatus* encompassing the early Lutetian—early Bartonian time span. Finally, sheets 505 Moliterno and 506 Sant'Arcangelo of the 1:50,000 official Italian geological map by ISPRA [5,6] indicated an early Miocene Age, based on data collected outside of the mapped areas. In the Trebisacce 1:50,000 sheet [46], which comprises the type-area of the Albidona Formation, an early Miocene age has been recognized, but only in the uppermost interval of the succession.

Difficulties in providing a consistent age of the Albidona Formation, combined with the paucity of key outcrops, have important consequences on the understanding of its paleogeographic significance as well as on the interpretation of its tectonic or stratigraphic relationships with the underlying units. According to a first interpretation [45,47], the basal contact of the Albidona Formation on the Apennine Platform and the Lagonegro Basin units, exposed in the southern sector of the high Agri Valley (Figure 1), has been indicated as an unconformity. An alternative interpretation [2] considers the same contact as a thrust surface and the Albidona Formation as deposited in a thrust-sheet top basin formed during the emplacement of the Liguride complex. Vezzani et al. ii [48] proposed a similar interpretation and considered the Albidona Formation as deposited in a thrust-sheet top basin that seals contractional structures affecting the Liguride accretionary wedge.

The first interpretation implies that at the time of deposition of the Albidona Formation the African paleomargin was already involved in the Apennine deformation. The second interpretation assumes that the Albidona thrust-sheet top basin formed on the Liguride accretionary wedge when the African paleomargin was still unaffected by contractional deformation. As the involvement of the African paleomargin in the Apennine chain took place during the early Miocene, according to the first deformation recorded in the Apennine

Platform and the Lagonegro Basin units [49,50], a more precise constrain on the age of the Albidona Formation would greatly help in solving this controversy and in providing new hints on the tectonic evolution of the southern Apennines. At this aim we analysed the stratigraphic organization of the Albidona Formation at Monte dell'Agresto, which is located along the southeastern side of the high Agri Valley.

4. Data and Methods

Detailed geological mapping at a 1:5000 scale of a 12.5 km^2 wide area, including the Costa Molina—Tempa del Vento—La Rossa—M. dell'Agresto localities, was performed in order to better understand the stratigraphy of the Albidona Formation and to analyse the structural setting of the area (Figure 2a). Mapping was focused on the identification of key stratigraphic horizons that have been correlated throughout the study area. After geological mapping, the most continuous and representative stratigraphic section (Figures 2b and 3) of the Albidona Formation, located at Coste dell'Agresto locality, was measured and sampled for biostratigraphic analysis on planktonic foraminifera and nannofossils. Other samples have been collected in significant outcrops of the area in order to better identify the age of the key horizons and to provide biostratigraphic constraints on some stratigraphic intervals of the Albidona Formation that were not represented in the measured stratigraphic section.

Analysis of calcareous nannofossils has been performed by means of standard smear slides prepared in the ENI laboratories of Bolgiano (San Donato Milanese). Semi-quantitative analyses of the assemblages were performed on a Zeiss Axioplan optical microscope. Okada and Bukry [51], Martini [52], Perch-Nielsen [53], Bown [54], Gradstein et al. ii [55], were used as standard references for the stratigraphic interpretation of nannofossil distribution.

Structural analysis has been focused on the description of fold geometry in the Albidona Formation and the documentation of the main fault zones. Large-scale folds affecting the Albidona Formation have been mapped by distinguishing the upright and overturned limbs and by identifying the trace of the fold axial surfaces. Overturned beds have been easily detected by means of classical way-up criteria used for turbidites. Brittle deformation has been analysed at Coste dell'Agresto locality, where the orientation of minor fault planes and fractures has been measured within one major fault zone of the study area. The number of fractures per unit length in the damage zones, defined as fracture intensity or P10 [56,57], has been estimated by means of linear scanlines.

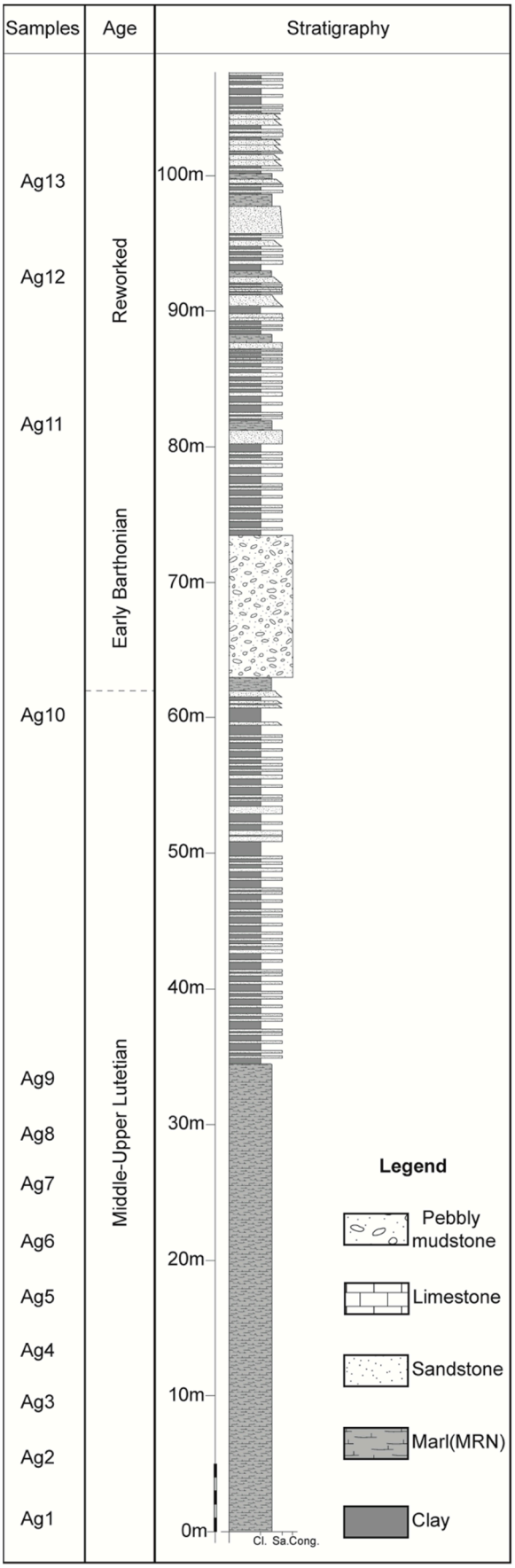

Figure 3. Stratigraphic section of the member B–C (Albidona Formation), measured in the Coste dell'Agresto locality.

5. Stratigraphy of the Monte Dell'agresto Area

We will describe the stratigraphic successions exposed at Monte dell'Agresto area (Figure 2a,b and Figure 3) adopting, for the Albidona Formation, the same stratigraphic divisions proposed by Baruffini et al. ii [33], defined in the Albidona type locality. The reason for this choice is the striking stratigraphical and chronostratigraphical similarities of the studied successions with the section exposed in the type locality. Baruffini et al. ii [33] identified four members in the Albidona formation: (i) member A, consisting of a turbiditic system made by coarse-grained sandstones and microconglomerates. Rare marly intervals locally alternate with the main lithologies; (ii) member B, made up of thick marly intervals (up to tens of metres), alternating with turbiditic sandstone beds and clay intervals. Thick conglomerate levels also occur; (iii) member C, consisting of marly clays and coarse-grained sandstones, with rare calciclastic levels; (iv) member D, mainly composed of coarse-grained turbiditic sandstones and conglomerates, with thin and rare calciclastic intervals.

In the Monte dell'Agresto area we recognized three of the four members described by Baruffini et al. ii [33]. However, the distinction between members B and C is not so straightforward as in the type-area; therefore, we decided to merge the two members together to form the member B–C. On the other hand, member D is easily distinguishable from the underlying members. Member A is not exposed in the study area.

5.1. Albidona Formation, Member B–C

The stratigraphic organization of the member B–C is visible in a natural section exposed along the southeastern slope of Monte dell'Agresto (Figure 3). Member B–C mainly consists of siliciclastic turbidites locally alternating with marly and calcareous intervals. The most common lithofacies, forming the background of the member B–C, is represented by alternating thin-bedded turbiditic sandstones and clays (Figures 3 and 4a).

Sandstones mainly consist of medium to fine—grained turbidites forming cm to dm-thick beds. They show marked erosional basal surfaces and sedimentary structures as well as the Ta-c intervals of the Bouma sequence [58]. The clays commonly form greyish to greenish m-thick, thinly laminated packages. Structureless sandstones in m-thick layers stand out at different stratigraphic heights within background sediments (Figure 4b). Often, the observed thickness of the sandstone beds is the result of amalgamation processes between different strata. Structureless sandstones commonly show lens-shaped geometry, marked erosional basal surfaces and clay chips, ripped up from the underlying clays. Further intercalations within the background deposits of the member B–C consist in three distinctive sedimentary bodies (Figures 3 and 4) that, for their uniqueness, represent very useful stratigraphic markers. These bodies form a triplet that can be traced for many kilometres throughout the study area.

The oldest is represented by a whitish marly interval, affected by cleavage, joints and calcite veins (Figure 4c), showing an anomalous maximum thickness of about 40 m. This interval represents not only an easily recognizable key bed but it also useful for biostratigraphic determinations, given its abundant faunal content (see the next section). Marly intervals occurring within the Albidona Formation have been interpreted as megaturbidites [35] or as "homogenites", possibly triggered by tsunami events [38].

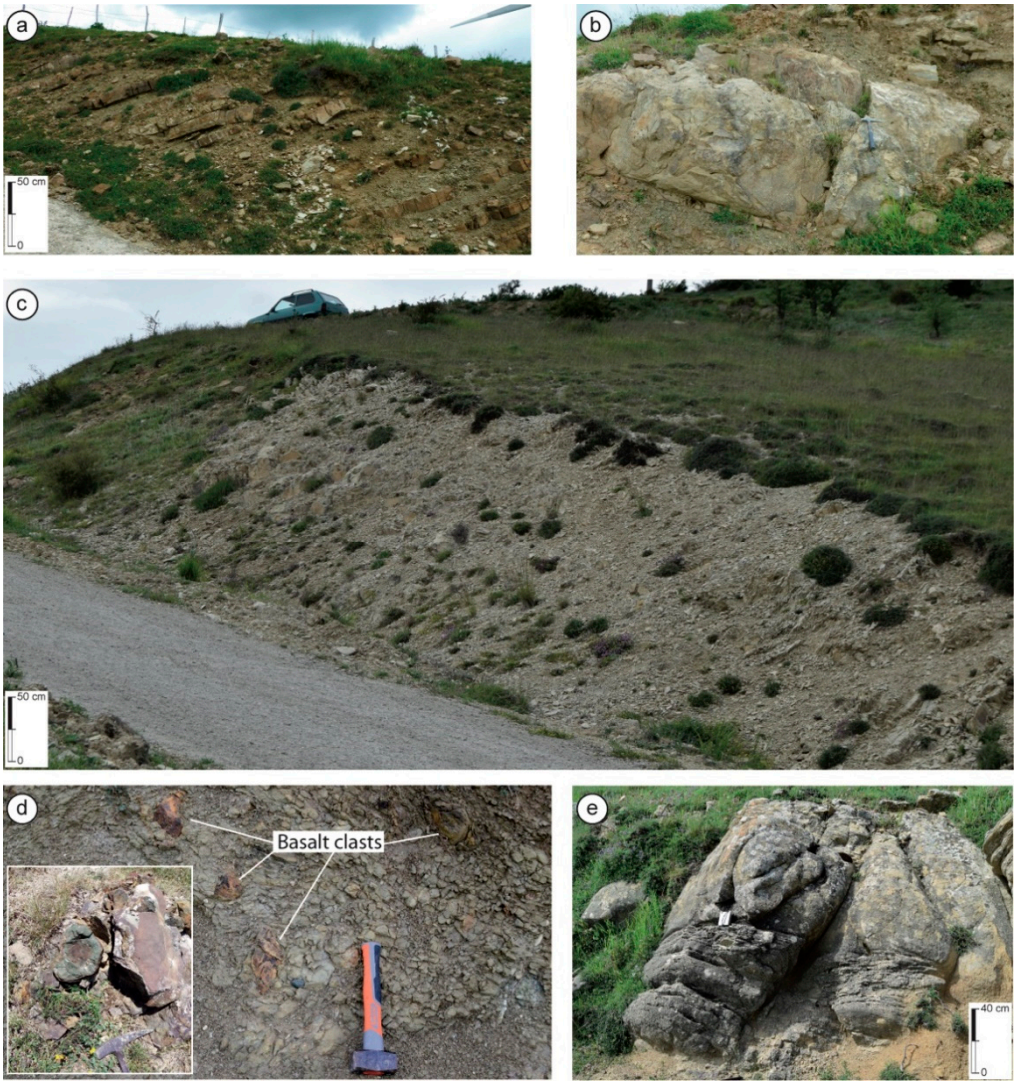

Figure 4. Photographs illustrating peculiar stratigraphic intervals within member B–C and D of the Albidona Formation. (**a**) Thin-bedded turbidites and clays representing the background sedimentation of member B–C of the Albidona Formation; (**b**) Structureless sandstone intervals; (**c**) Marls affected by cleavage and calcite veins; (**d**) Pebbly mudstone exposed at Monte dell'Agresto. Note the occurrence of scattered basalt clasts within the clayey matrix. In the box, a close-up view of pillow lava fragments; (**e**) Pebbly sandstone. Scattered clasts mainly occur in the laminated lower portion.

A second key level, located about 30 m above the described marls, is represented by an about 10 m-thick pebbly mudstone (Figures 3 and 4d), consisting of angular to sub-rounded pebbles and boulders dispersed within a greenish to greyish silty clay. Clasts consist of magmatic, metamorphic and sedimentary rocks. Magmatic rocks are mainly represented by white and pink granites, porphyries, microgabbros and black to green basalts.

Locally, fragments of pillow lavas (Figure 4d), with minor inter-pillow sediments, have been recognized. Metamorphic clasts are commonly represented by phyllites, schists and paragneisses, possibly overprinted by contact metamorphism. Sedimentary clasts are represented by rare Paleocene-Eocene carbonate platform limestones, greenish and reddish cherts and sandstones. Microfacies of carbonate clasts, indicating a reefal environment, is not consistent with the typical Eocene limestones of the Apennine Platform, represented by the shelf-lagoonal facies of the Trentinara Formation [59]. In general, clasts composition is consistent with the provenance from the upper part of a continental crust, where phyllites and schists are intruded by granitoids, covered by porphyres and, finally,

by platform carbonates. Moreover, the widespread occurrence of pillow lava fragments and microgabbro implies the presence of a second sedimentary source, consisting of an obducted ophiolitic complex. This is further supported by the concomitant occurrence of inter-pillow limestones and greenish to reddish cherts that typically occur in the upper part of an ophiolite section. Due to bad outcrop conditions pebbly mudstone did not show evident sedimentological characteristics and clear relationships with the surrounding strata. A possible interpretation, due to its structureless appearance, with clasts floating in a dominant clayey matrix, is that they result from the emplacement of a debris flow. This stratigraphic level might be correlated with similar intervals containing blocks of granitoids and mafic rocks exposed in various localities along the southwestern side of the Agri Valley [36,45,60].

The third marker bed is a pebbly sandstone (Figure 4e), which is located some metres above the pebbly mudstone. It consists of a 2–3 m-thick coarse-grained sandstone body showing well-rounded, a few centimetres in diameter, crystalline and metamorphic clasts distributed along the lower portion of the bed. Plane-parallel and cross-lamination typically occur in the basal portion of the bed, where the clasts are mostly present. Toward the top, clast frequency and lamination progressively decrease, and the sandstone become structureless or show a faint normal gradation. It shows a lens-shaped geometry and progressively pinches out eastward. In the opposite direction it can be followed for some kilometres, forming an easily recognizable marker bed. We interpreted the pebbly sandstone as the result of a turbidite flow or a debris flow evolving toward a turbidite flow.

5.2. Albidona Formation, Member D

Member D differs from member B–C mainly for two reasons: (i) fine to medium grained sandstones are replaced by coarse-grained sandstones, micro-conglomerates and conglomerates (Figure 5a,b); (ii) Marly intervals are thinner and commonly show higher clay content.

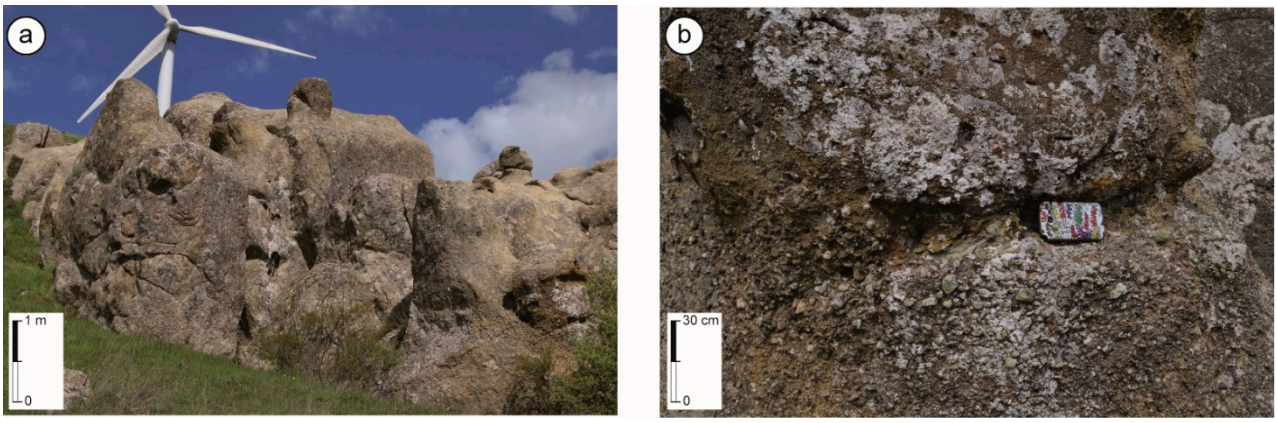

Figure 5. (**a**) Typical outcrops of the member D of the Albidona Formation represented by thick conglomerate/micro-conglomerate beds; (**b**) Close-up view of the conglomerates.

The conglomerate/micro-conglomerate beds show thicknesses ranging from few centimetres to some metres and can be followed laterally for hundreds of metres. They commonly show a lens-shaped geometry, dome-shaped tops and marked erosional basal surfaces. Conglomerate/micro-conglomerate beds display a matrix-supported texture with clast size ranging from few centimetres up to the decimetre. Clast roundness can vary from scarcely rounded to well rounded. Clast composition includes sedimentary, magmatic and metamorphic rocks. Among metamorphic rocks, well-rounded clasts of quartz veins and subrounded phyllite fragments are the most frequent, whereas magmatic rocks mainly consist of granite clasts. Unlike the member B–C, apparently they do not include ophiolite-derived debris.

Marls of member D show general features similar to those described for the underlying member B–C; however, they are characterized by a greater amount of clay and, consequently by paucity in faunal content. Marls are commonly organized in laterally continuous beds showing thicknesses ranging from some tens of centimetres to some meters and are generally affected by an intense cleavage, commonly parallel to the sedimentary layering.

5.3. Gorgoglione Formation

The Gorgoglione Formation (late Burdigalian—Tortonian according to [61]) mainly consists of arenaceous turbidites, variably alternated with matrix-supported conglomerate/microconglomerate layers and clay-rich intervals. In the study area arenaceous turbidites consist of 1–2 m thick coarse-grained graded sandstone, containing sparse clasts at the base and laminated finer-grained sandstone on top. Conglomerates generally consist of rounded clasts derived from sedimentary, metamorphic and igneous rocks, these latter showing a granite to granodiorite composition, within abundant matrix. Sandstones and conglomerates are generally characterized by a yellow color, may contain plant remains and are frequently organized in 10 to 50 m thick intervals. Minor cm- to dm-thick clayey intervals alternate with the previous lithologies. Frequently, thick sandstone and conglomerate intervals result from the amalgamation of individual m-thick turbidite levels. These coarse-grained intervals are laterally discontinuous and occur within a typical turbiditic sequence, consisting of dm-thick layers of graded sandstone intercalated within dominant clay or silty clay.

Interestingly, the Gorgoglione Formation never contains marly intervals, and this represented one of the main criteria that we used for distinguishing the Gorgoglione Formation from both B–C and D members of the Albidona Formation. Another distinctive feature is the exclusive presence of pebbles consisting of granitoids and minor metamorphic rocks in the coarse-grained facies, with the absence of ophiolitic material.

6. Biostratigraphy

In the Monte dell'Agresto area 31 samples were collected for the biostratigraphic analysis of the Albidona Formation succession. Samples have been mainly collected in marly intervals located at different stratigraphic heights, within both the B–C and the D members. They have been organized in three main groups representing, respectively, the intermediate and lower-intermediate intervals of the member B–C (Groups I and II; Tables 1 and 2), and the member D (Group III; Table 3). The samples are characterized by the significant occurrence of Cretaceous, Paleocene reworked forms. In addition, the constant occurrence of Eocene forms, not older than the Lutetian, has been ascertained by integrating calcareous nannoplankton and planktonic foraminifera. Although forms with a long-range distribution (i.e., *Chiloguembelina cubensis*, LO top Rupelian, *Sphenolithus praedistentus*, LO intra-Chattian) sometimes occur, we never recognized taxa with a short range distribution or a FO/FAD showing ages younger than lower Priabonian (i.e., *Cribrocentrum erbae*). Therefore, based on comparison between marker planktonic foraminifera and calcareous nannoplankton associations (Figure 6) we attributed of a Lutetian age for the member B–C and a Barthonian/early Priabonian age for the member D.

Table 1. Group I.

Samples	Markers (Calcareous Nannoplankton)	Markers (Plantktonic Foraminifera)
AG 28	*Sphenolithus radians*, *Girgisia gammation*, *Toweius pertusus*, *Discoaster barbadiensis* Sample biostratigraphic range: NP11–14	*Acarinina* cf. *topilensis*, *Chiloguembelina* sp., *Turborotalia* sp. Sample biostratigraphic range: E10–E11
AG 27	*S. radians*, *G. gammation*, *T. pertusus*, *D. barbadiensis* Sample biostratigraphic range: NP11–14	*Acarinina* cf. *boudreauxi*, *Morozovelloides* sp.? *Chi-loguembelina* sp., *Subbotina* spp., *Globigerinatheka* sp., *Morozovella* cf. *caucasica*, Globotruncanidae (rew.) Sample biostratigraphic range: E10–E11
AG 15	*S. radians*, *G. gammation*, *Toweius callosus*, *T. pertusus* Sample biostratigraphic range: NP11–14	Barren
AG 14	*S. radians*, *G. gammation*, *T. callosus*, *T. pertusus* Sample biostratigraphic range: NP11–14	Barren
AG 13	*S. radians*, *G. gammation*, *Sphenolithus orphanknollensis*, *Nannotetrina* sp., *D. barbadiensis* Sample biostratigraphic range: NP12–15	Barren
AG 12	*S. radians*, *G. gammation*, *S. orphanknollensis*, *Nannotetrina* sp., *D. barbadiensis* Sample biostratigraphic range: NP12–15	Very rare indeterminated planktonic foraminifera
AG 11	*S. radians*, *G. gammation*, *S. orphanknollensis*, *Nannotetrina* sp., *D. barbadiensis* Sample Biostratigraphic range: NP12–15	Barren
AG 10	*S. radians*, *G. gammation*, *S. orphanknollensis*, *Nannotetrina* sp., *D. barbadiensis* Sample biostratigraphic range: NP12–15	Rare indeterminated planktonic foraminifera
AG 9	*Sphenolithus predistentus*, *Helicosphaera lophota*, *G. gammation* Sample Biostratigraphic range: NP16	Barren
AG 8	*generic Eocene association*	*Acarinina* spp. and small indeterminated planktonic foraminifera
AG 7	*Sphenolithus spiniger*, *Sphenolithus furcatolithoides* Sample biostratigraphic range: NP15/16	*Morozovella aequa* (rew.), *Acarinina soldadoensis* (rew.) Sample biostratigraphic range: not younger than E7
AG 6	*S. radians*, *G. gammation*, *S. furcatolithoides*, *D. barbadiensis* Sample biostratigraphic range: NP15	*Acarinina bullbrooki*, *Acarinina* spp. Sample biostratigraphic range: E7–E11
AG 5	*S. radians*, *G. gammation*, *T. pertusus*, *T. callosus* Sample biostratigraphic range: NP11–14	*Acarenina* cf. *soldadoensis* (rew), *Morozovella aragonensis* Sample biostratigraphic range: E7–E11
AG 4	*S. radians*, *G. gammation*, *T. pertusus*, *T. callosus* Sample biostratigraphic range: NP11–14	*Acarinina* sp., *Morozovella* sp. Sample biostratigraphic range: not younger than E9
AG 3	*S. radians*, *G. gammation*, *T. pertusus*, *T. callosus* Sample biostratigraphic range: NP11–14	*Acarinina bullbrooki*, *Subbotina* spp., *Globanomalina* cf. *compressa* (rew.) Sample biostratigraphic range: E7–E11
AG 2	*S. radians*, *G. gammation*, *T. pertusus*, *T. callosus* Sample biostratigraphic range: NP11–14	*Acarinina* sp., *Morozovella* sp. Sample biostratigraphic range: not younger than E9
AG 1	*S. radians*, *G. gammation*, *T. pertusus*, *T. callosus* Sample biostratigraphic range: NP11–14	*Acarinina bullbrooki*, *Subbotina* spp., *Morozovella* spp. Sample biostratigraphic range: E7–E11

Table 2. Group II.

Samples	Markers (Calcareous Nannoplankton)	Markers (Plantktonic Foraminifera)
AG 18	*S. spiniger* Sample biostratigraphic range: NP16	*Acarinina* cf. *boudreauxi* Sample biostratigraphic range: E7–E9
AG 17	*S. spiniger* Sample biostratigraphic range: NP16	*Acarinina* spp., *A.* cf. *pentacamerata* (rew.), *A. soldadoensis* (rew.), *Chiloguembelina* cf. *cubensis* Sample biostratigraphic range: E10 or younger
AG 22	*Discoaster salisburgensis*, *S. radians*, *G. gammation* Sample biostratigraphic range: NP11–12	*Acarinina* spp., *A.* cf. *bullbrooki*, *A. soldadoensis* (rew), *Globanomalina* sp. (rew.) Sample biostratigraphic range: E7–E11
AG 21	*D. salisburgensis*, *S. radians*, *G. gammation* Sample Biostratigraphic range: NP11–12	*Acarinina* spp., *A.* cf. *boudreauxi*, *Acarinina soldadoensis* (rew), *Igorina* sp. (rew.), *Morozovella aequa* (rew.) Sample biostratigraphic range: E7–E11
AG 20	*S. radians*, *G. gammation*, *T. callosus*, *T. pertusus* Sample biostratigraphic range: NP11–14	*Acarinina* spp., *A.* cf. *boudreauxi*, *Acarinina soldadoensis* (rew), *Chiloguembelina crinita*, *Morozovelloides* sp.? *Subbotina* spp. Sample biostratigraphic range: E7–E13
AG 19	*S. radians*, *G. gammation*, *T. callosus*, *T. pertusus* Sample biostratigraphic range: NP11–14	*Acarinina* spp., *A.* cf. *boudreauxi*, *A. pentacamerata* (rew), *Chiloguembelina* spp., *Igorina pusilla* (rew.) Sample biostratigraphic range: E7–E9
AG 30	*S. radians*, *G. gammation*, *Campylosphaera dela*, *Discoaster saipanensis* *D. barbadiensis* Sample biostratigraphic range: NP14	Very rare small planktonic foraminifera fragments
AG 31	*S. radians*, *G. gammation*, *C. dela*, *D. saipanensis*, *D. barbadiensis* Sample biostratigraphic range: NP14	No sample
AG 32	*S. radians*, *G. gammation*, *T. callosus*, *T. pertusus* Sample biostratigraphic range: NP11–14	No sample
AG 33	*S. radians*, *G. gammation*, *T. callosus*, *T. pertusus* Sample biostratigraphic range: NP11–14	*Acarinina bullbrooki*, *A.* cf. *aspensis*, *Globigerinatheka* sp., Chiloguembelina sp., *Morozovella* spp., *M. aequa* (rew.), *Globanomalina compressa* (rew.), *Igorina albeari* (rew.) Sample biostratigraphic range: E7–E11

Table 3. Group III.

Samples	Markers (Calcareous Nannoplankton)	Markers (Plantktonic Foraminifera)
AG 26	*Cribrocentrum reticulatum*, *Dictyococcites bisectus*, *Reticulofenestra umbilicus*, *Sphenolithus obtusus*, *Cribrocentrum erbae* Sample biostratigraphic range: NP17	Barren
AG 25	*Cr. reticulatum*, *D. bisectus*, *R. umbilicus*, *S. obtusus*, *Cr. erbae*, *Blackites* sp. Sample biostratigraphic range: NP17	Barren
AG 24	*Cr. reticulatum*, *D. bisectus*, *R. umbilicus*, *S. obtusus*, *Cr. erbae*, *Blackites* sp. Sample biostratigraphic range: NP17	Barren
AG 23	*Cr. reticulatum*, *D. bisectus*, *R. umbilicus*, *S. obtusus*, *Cr. erbae*, *Blackites* sp. Sample biostratigraphic range: NP17	Barren

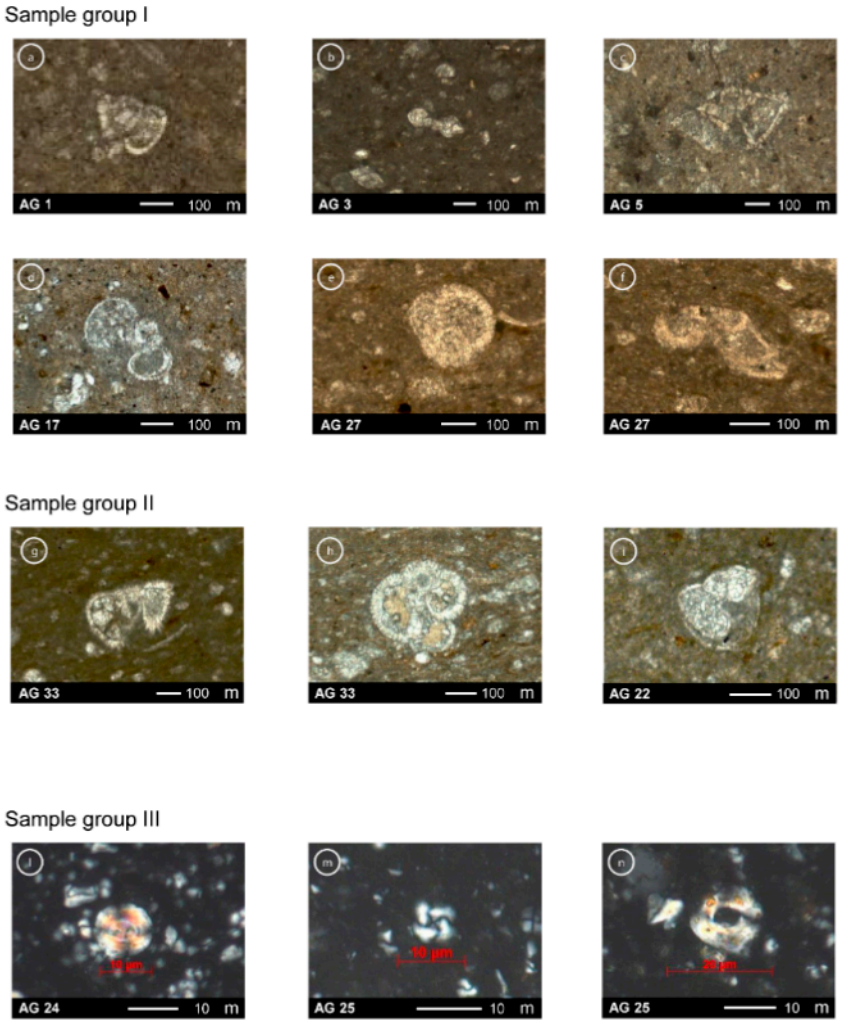

Figure 6. Sample group I: (**a**) *Acarinina bullbrooki*; (**b**) *Globanomalina* cf. *compressa* reworked; (**c**) *Morozovella aragonensis*; (**d**) *Acarinina soldadoensis* reworked; (**e**) *Globigerinatheka* sp.; (**f**) Globotruncanids (*Marginotruncana* sp.?) reworked; Sample group II: (**g**) *Acarinina bullbrooki*; (**h**) *Globigerinatheka* sp.; (**i**) *Turborotalia* sp. (juvenile); Sample group III: (**l**) *Dictyococcites bisectus*; (**m**) *Cribrocentrum reticulatum*; (**n**) *Reticulofenestra umbilicus*.

6.1. Group I

This group consists of a composite succession representative of the member B–C of the Albidona Formation, exposed northern sector of the study area (Figure 2). It includes samples from AG1 to AG13, collected at Coste dell'Agresto along the measured stratigraphic section (Figure 3), and samples AG14-15 and AG27-28 from minor marly intervals in the same area. In particular, the previously described marly key level (MRN interval in Figure 3) has been sampled at regular distances of 4–5 m (samples AG1-9; Figure 3). In the sampled marly intervals (Table 1), calcareous nannoplankton associations are abundant and well preserved. On the contrary planktonic foraminifera associations, analysed in thin sections, are scarcely represented and some of the samples resulted barren. In general, the existing forms are small, well preserved and iso-oriented. In some samples radiolarians are abundant. Information and marker forms for each sample are reported in Table 1. The most representative specimens recognized in this group are illustrated in Figure 6a–f.

Group I encompasses the middle-upper Lutetian (Biozones NP15-16) (see the chronostratigraphic scheme in Figure 7). The first form representative of the nannoplankton Biozone NP15 is *Sphenolithus furcatolithoides*, observed in the sample AG6. Furthermore, *Sphenolithus predistentus*, indicating the transition toward the Biozone NP16, has been rec-

ognized in sample AG9. A Lutetian age is also confirmed by the occurrence of planktonic foraminifera as well as *Acarinina* cf. *topilensis*, *Globigerinatheka* sp. recognized in the samples AG27 and AG28.

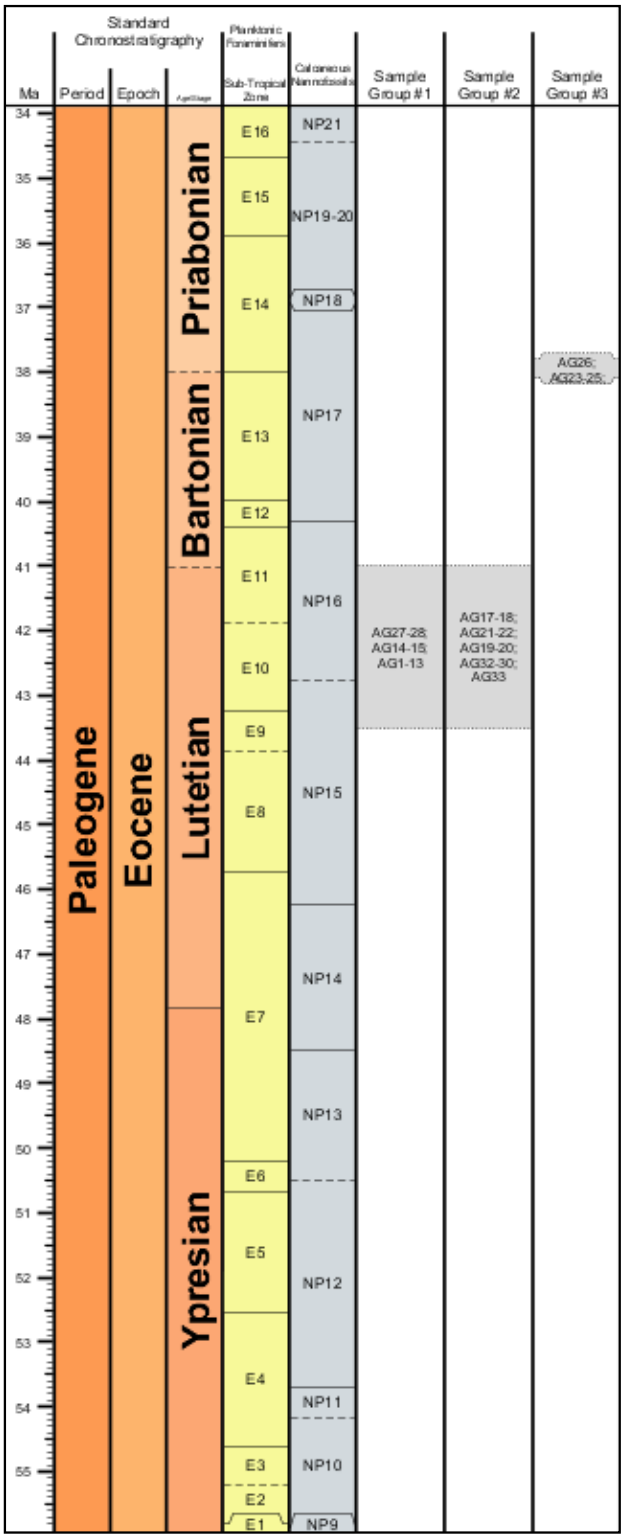

Figure 7. Final interpretative chronostratigraphic scheme reconstructed for the study succession. Reworked Ypresian and older bioevents are often present in samples.

In the other samples the age attribution is less clear since reworked forms are very common. In general, reworked planktonic foraminifera of Cretaceous, Paleocene and late Ypresian (i.e., *Acarinina soldadoensis*, *Morozovella aequa*) ages are present. Large range forms or markers ranging from nannoplankton biozones NP11 and NP24 also occur. In particular, the recognition of *Sphenolithus predistentus*, which ranges from biozone NP16 to biozones NP24 at least provided an age not older than biozone NP16. Although this latter form can easily reach the Oligocene we exclude this younger age because of the lack of a clear Oligocene faunal assemblage.

In more detail, samples AG1-AG5, collected at the base of the MRN interval, show fossil assemblages that do not allow to exclude a late Ypresian age. In fact, the occurrence of *Acarinina bullbrooki* in the sample AG1 provides an age not older than E7 biozone. Accordingly, calcareous nannoplankton associations indicate an age not younger than NP14 biozone. The occurrence of calcareous nannoplankton associations pertaining to the biozone NP15 in the sample AG6 might suggest that the underlying stratigraphic portions can be located in the upper part of the NP14 biozone and therefore in the Lutetian. The occurrence of *Sphenolithus predistensus* (total range NP16-NP24) allows to attribute the sample AG9 at the base of NP16 Biozone. In this sample, the fossil assemblage is also characterized by a group of taxa of lower Eocene affinity such as *Girgisia gammation* (total range NP11-NP14), always observed in the underlying samples. These latter forms could be interpreted as clearly reworked only from the sample AG6, due to the first occurrence of *Sphenolithus furcatulithoides* (total range NP15-16).

The aforementioned biostratigraphic reconstruction might suggest that the 34 m thick MRN interval could represent a condensed section ranging between the upper Ypresian? and the upper Lutetian (NP14-16). However, the MRN interval is included in a thick turbidite succession characterized by high sedimentation rates. Therefore, a prolonged deactivation of the clastic input (6–7 My) during deposition of the MRN interval seems unlikely. Moreover, it has to be noted that samples collected from marly levels overlying the MRN interval show again fossil associations with upper Ypresian—lower Lutetian affinities, similar to those recognized in the samples AG1-AG5. The occurrence of these intervals has been attributed to reworking processes, only occasionally preserving the primary biostratigraphic signal (samples AG 27—AG28). The recurring appearance of layers containing calcareous nannoplankton associations with an upper Ypresian—lower Lutetian (NP11-14) affinity, conflicting with their stratigraphic position in the Agresto succession, rises further doubts about the reliability of the age provided by samples AG1-AG5. For these reasons, the stratigraphic interval included between samples AG1 and AG5 has been assigned to the Lutetian (biozone NP15).

6.2. Group II

Group II consists of a composite succession representative of the member B–C of the Albidona Formation exposed central sector of the study area. It includes samples AG17-18-19-20-21-22-30-32-33 (Figure 2). Samples AG19-20-21-22 have been collected along the MRN marker interval (Figures 2 and 3). The most representative forms are listed in Table 2. Figure 6g–i show the most representative forms of this group.

Consistently with the samples of Group I, a Lutetian age is ascertained for Group II and abundant reworked forms of Cretaceous, Paleocene and Ypresian age have also been recognized. In particular, the reworked nature of early Eocene forms is similar to that discussed for the Group I.

Planktonic foraminifera represented by *Globigerinatheka* spp. recognized in the sample AG33 provided a Lutetian age not older than Biozone E8. Moreover, sample AG17, located above the MNR interval, provided and age not older than Biozone E10 (topmost NP15-NP16), because of the occurrence of *Chiloguembelina* cf. *cubensis*.

Summing up, we indicate an age comprised between the upper part of NP15 and the lower part of NP16 calcareous nannoplankton biozones, corresponding to E9-E10 planktonic foraminifera biozones for Group I and Group II samples (Figure 7). Therefore,

the studied stratigraphic interval corresponds to a minor part of the entire Albidona member B–C, which is characterized by high sedimentation rates and a thickness of 1500 m in the type locality [33].

6.3. Group III

This group includes samples AG 23-24-25 (Figure 2), collected in a marly interval of the member D of the Albidona Formation. Additionally, sample AG26 has been attributed to this group, and referred to the same member, because of the strong affinities showed by the floral content with the other samples of Group III. Calcareous nannoplankton associations are abundant and very well preserved (Figure 6l–n). On the contrary, planktonic foraminifera content is almost absent. The occurrence of markers as *Blackites* sp., *Cribrocentrum erbae*, *Cribrocentrum reticulatum*, *Dictyococcites bisectus*, *Reticulofenestra umbilicus*, *Sphenolithus obtusus*, allowed to refer Group III to the topmost Barthonian/lower Priabonian (Biozone NP17) (Figure 7).

7. Structural Setting of the Monte dell'Agresto Area

The detailed stratigraphic reconstruction of the Albidona Formation and the identification of key stratigraphic intervals allowed a better definition of the overall geological features of the study area, which appear substantially upgraded when compared with the previous geological maps [3,5,6]. The most striking characteristics is that most of the previously mapped Gorgoglione Formation turned out to be the Albidona Formation (Figure 2). This information was crucial for identifying major tectonic contacts that separate the two formations in most of the study area. Another important improvement consists in the distinction of members B–C and D of the Albidona Formation, which allowed a more detailed mapping of this thick and sometimes monotonous succession. These advancements allowed the identification of two roughly SW-NE oriented major faults, crossing the entire study area, named, respectively, as the Figliarola and Tempa del Vento faults. These two faults crosscut older contractional structures, represented by folds, which formed during the building of the southern Apennine thrust belt. In the next sections we will describe the main contractional and extensional structures recognized in the study area.

7.1. Contractional Structures

Contractional tectonics in the study area is mainly outlined by the presence of folds at the meso- and macro-scale. Minor thrusts and reverse faults, generally characterized by a limited displacement (up to some metres), also occur. We observed a remarkable difference in the folding style between the members B–C and D. In particular, in the member B–C folds are more commonly open and upright, which is very likely controlled by the occurrence of more than 10 m thick layers, represented by the marly key interval and by thick sandstone beds. On the contrary, folds in the member D show a tighter geometry, related to the predominance of thinner sandstone or microconglomerate layers.

7.1.1. Geometry and Orientation of Folds in the Member B–C

Folds in the member B–C consist of roughly NW-SE oriented anticlines and synclines. Fold orientation has been deduced by plotting the poles of the bedding planes (stereoplot A and B; Figure 8) that, although dispersed, are consistent with a best fit axis dipping of about 45° to 300° N.

Coherent with this orientation is an open NW-trending anticline recognized along the southern side of Coste dell'Agresto locality (Figure 2), which is outlined by a thick sandstone interval and by the marly key bed (Figure 9a). In the same locality, overturned minor folds also affect the member B–C. These structures commonly show axes dipping toward W of 20° (Figure 2) and, due to their orientation and asymmetry, are not consistent with the dominant large-scale NW-trending folds detected within the member B–C. Consequently, these structures probably pertain to different deformation stage.

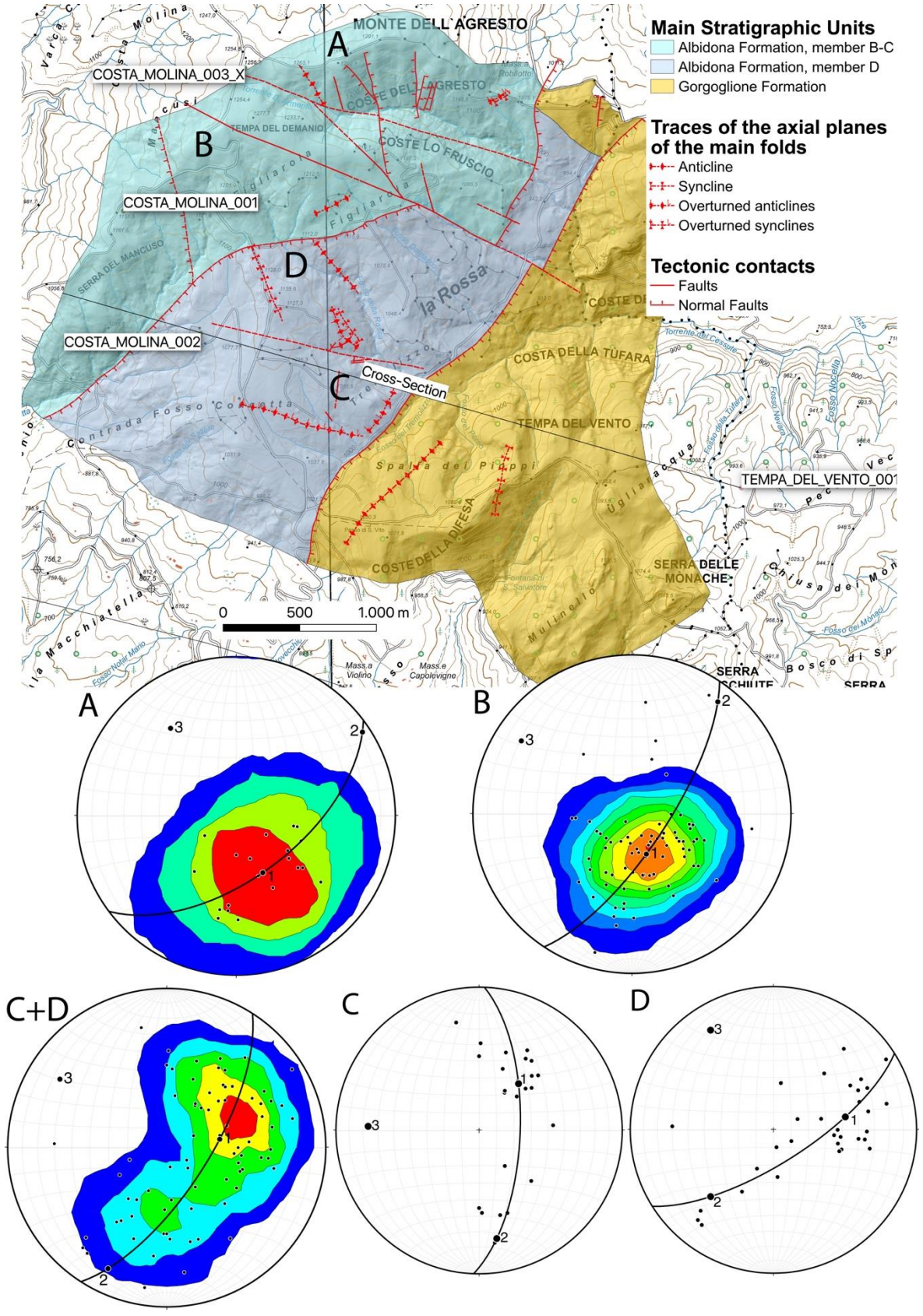

Figure 8. Tectonic sketch map of the study area. *Stereoplots* show the distribution of the bedding poles in the sub-areas **A**–**D**. The dot 3 corresponds with the *best-fit* axis of the folds.

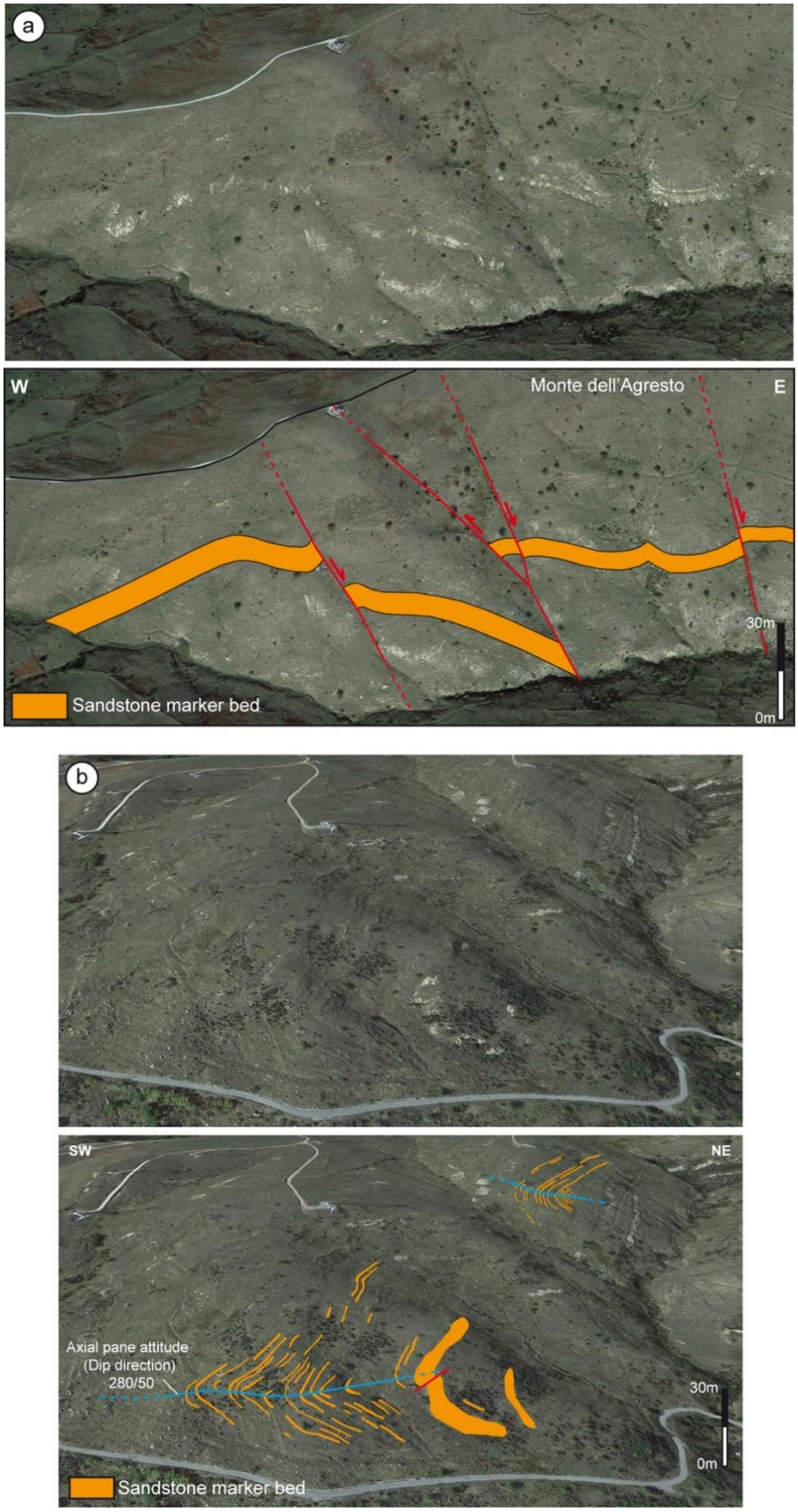

Figure 9. Examples of tectonic structures exposed in the M. dell'Agresto—C.da La Rossa area. (**a**) NW-trending anticline outlined by a thick sandstone bed at M. dell'Agresto; (**b**) Geometry of the E-trending Tremolizzo overturned anticline. Pictures from Google Earth.

7.1.2. Geometry and Orientation of Folds in the Member D

Similar to the previous case, folds in the member D consist of anticlines and synclines showing NW-SE and E-W hinge directions (stereoplot C and D in Figure 8). They generally consist of tight folds, often overturned, affecting interbedded clay, sandstone and microconglomerate. Hinge zones, where exposed, commonly show an angular to sub-angular geometry. A major E-W trending kilometre-scale overturned anticline crops out at Tremolizzo. The fold shows an axis plunging 20° towards N278. In the same locality, the presence of evident and angular fold hinges (Figure 9b) allows to appreciate an axial surface dipping of about 20–30° to the west (N280), consistent with the westward plunge of the fold axis. The same anticline can be mapped eastwards, between Tremolizzo and the Costa Molina, where the north-dipping overturned limb is well exposed (Figure 2). Interestingly, in the Costa Molina area the fold axial surface dips approximately to the east, indicating that the Tremolizzo anticline has been refolded by a gentle NW-trending syncline, generating a type 2 interference structure [62]. The overall geometry of the Tremolizzo anticline, characterized by an overturned southern limb, clearly indicates a southward-directed vergence, not consistent with the general northeastward thrust transport direction displayed by the Southern Apennine belt. Similar E-W trending asymmetric folds are present in other outcrops in the study area, where in some cases display hinge collapse phenomena and layer-parallel shearing.

Summarizing, interference structures in member D document that the Albidona Formation has been affected by at least two folding phases. The first phase (D1) consists of asymmetric and frequently overturned folds with southward transport direction. The second folding phase (D2) is generally characterized by NW-trending open folds (Figure 8; stereoplot D), with local overturned beds.

7.2. Extensional Structures

Three main fault sets, oriented, respectively, NNE-SSW, NW-SE and WNW-ESE have been recognized throughout the study area (Figure 2). Due to the poor outcrop conditions, in most cases fault have been inferred by the offset of marker levels or on the basis of stratigraphic inconsistency. In rarer cases, outcropping, meso-scale fault planes have been observed and measured. Considering the NE-SW set, two major kilometre-scale faults, named, respectively, Tempa del Vento and Figliarola faults, have been detected. Their occurrence has been mainly deduced on the basis of key beds offset and on the geometrical relationships between the mapped stratigraphic units. However, the presence of both faults is locally documented by exposures of the fault zones and is confirmed by the analysis of seismic lines acquired for hydrocarbon exploration in the area.

The Tempa del Vento Fault (Figure 2) is a NNE-SSW oriented and ESE-dipping normal fault, which separates the member D of the Albidona Formation at the footwall from the Gorgoglione Formation at the hangingwall. The main evidence for the presence of the fault comes from the geometrical relationships between the two formations and, particularly, from the attitude of the bedding planes in the Gorgoglione Formation, which dips constantly of 30° to towards Albidona Formation at the footwall. Tilting of the Gorgoglione Formation is consistent with the geometry of the downthrown block of a normal fault and supports the extensional kinematics of the Tempa del Vento Fault. The presence of the Gorgoglione Formation at the footwall of the fault in the northeastern sector of the study area suggests a gradual decrease of the vertical displacement towards the northeast.

The Figliarola Fault consists in two segments, oriented NE-SW and NNE-SSW, respectively, with a general dip towards the SE. This normal fault shows the deposits pertaining to the member B–C of the Albidona Formation at the footwall and the member D of the Albidona Formation plus the overlying Gorgoglione Formation at the hangingwall. The fault consists of a poorly exposed master fault plane and series of closely spaced, mostly antithetic minor faults. It shows a wide damage zone clearly exposed along the eastern side of Monte dell'Agresto. The damage zone affects a 15 m thick sandstone and microcon-

glomerate layer pertaining to the Gorgoglione Formation, located at the hangingwall of the structure. Fracture measurement carried out in this outcrop are showed in Figure 10a,b Three main fracture sets have been recognized, two of them, showing a NNE-SSW strike and dipping, respectively, toward WNW and ESE, form a conjugate fracture system which is consistent with the orientation and the extensional kinematics of the Figliarola Fault. A third set strikes NNW-SSE and dips steeply towards the WSW. A scanline measured orthogonally to the conjugate fracture set, along a 16 m long exposure, allowed to evaluate the fracture intensity (P10) [56,57]. As showed in Figure 10c the fracture intensity progressively decreases in a direction opposite to the master fault, which is located on the on the left-hand side of the histogram, showing a good agreement with the distribution of fractures in damage zones [63,64]. Isolated peaks occurring, respectively, at 8, 12 and 15 m, coincides with the presence subsidiary faults within the damage zone.

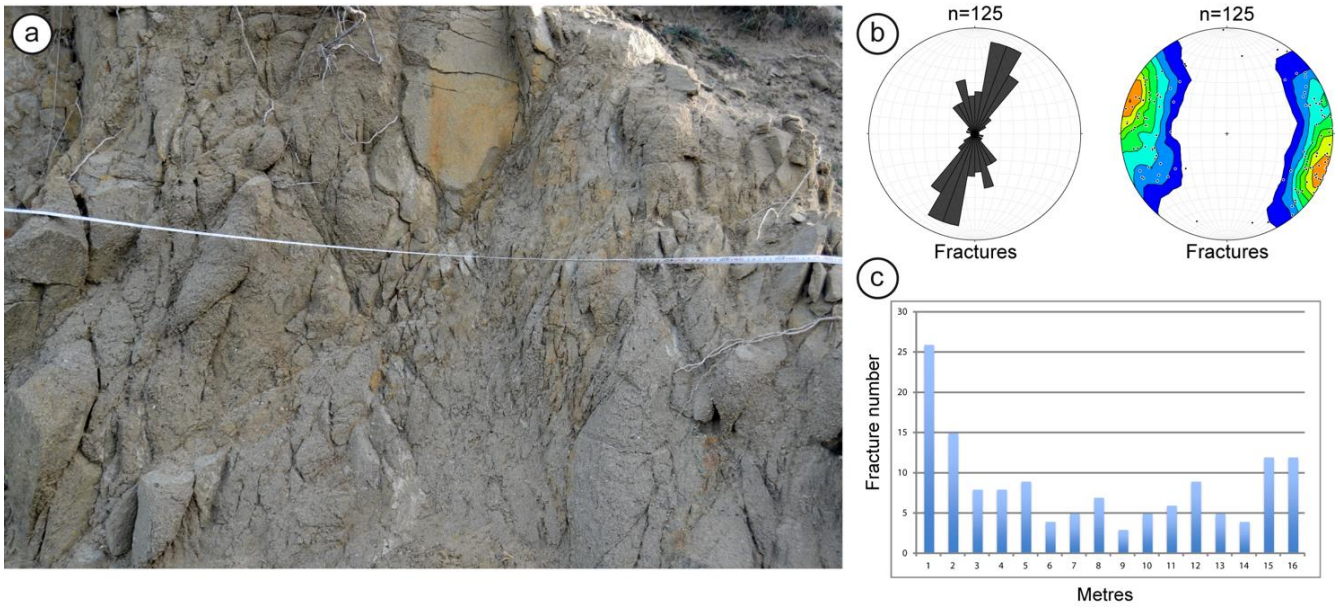

Figure 10. Structural data from the damage zone of the Figliarola Fault. (**a**) close up outcrop photograph; (**b**) rose and contour plot diagrams of fracture data measured along the scanline shown in (**a**); (**c**) distribution of the fracture intensity along the scanline shown in (**a**). Master fault is located at the left end side of the histogram.

At the hangingwall of the Figliarola Fault a series of antithetic, meso-scale faults also occur in an outcrop located 400 m East from the master fault (Figure 2). These structures cut through the Gorgoglione Formation deposits which, in this area, consist of thick beds of yellowish sandstone alternating with thin clay intervals (Figure 11a). Faults are oriented 10° N–20° E, with an average dip angle of 60°, and show displacements ranging from few decimetres to a minimum of 3 m and spacing varying form few decimetres to some meters. Fracture intensity within the fault-bounded blocks has been analysed by means of two scanlines (Figure 11b) that have been oriented parallel to the two main sandstone beds. Histograms (Figure 11c) show high values of fracture intensity approaching the fault A, which is characterized by the maximum displacement, and in the central part of the outcrop, where the closely spaced faults C and D bound a narrow sandstone block. Fractures are oriented NNE-SSW in average, which is consistent with the orientation of the minor antithetic faults and of the Figliarola master fault and appear arranged into two conjugate sets, showing dip angles of 45–55° (Figure 11d). Less commonly, a third set showing steeper dip angles can be detected (Figure 11d).

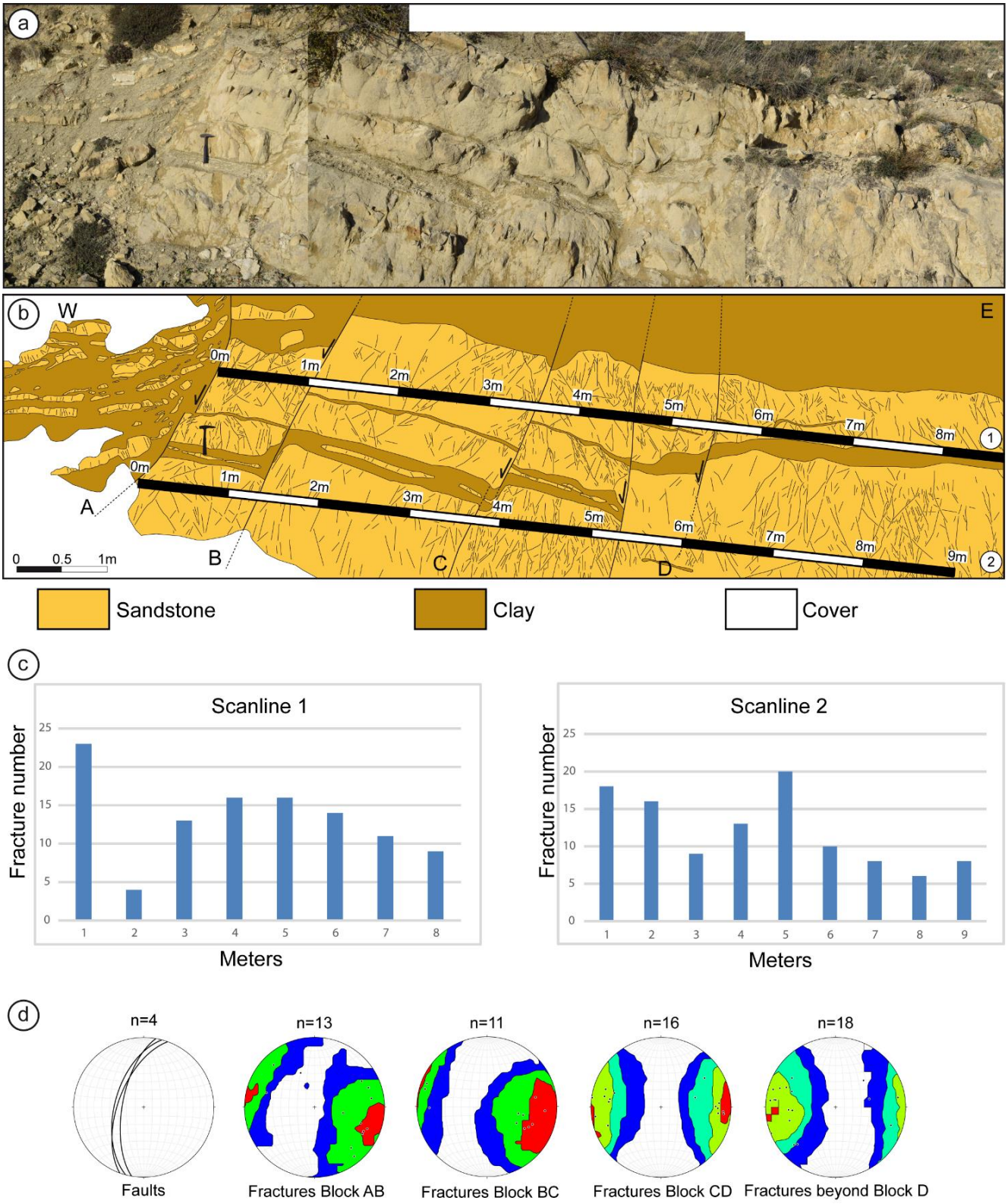

Figure 11. Minor antithetic faults, identified by letters A to D, in the Gorgoglione Formation exposed at the hangingwall of the Figliarola Fault. (**a**) outcrop photograph; (**b**) interpretation showing the position of two scanlines measured along two main sandstone beds; (**c**) diagrams of the fracture intensity measured along the two scanlines; (**d**) stereoplots showing the orientation of fault planes and fractures in each fault-bounded block shown in (**b**).

Seismic Profiles

A series of seismic profiles, acquired during exploration of the Val d'Agri oil field by ENI, provide support on the subsurface geometry of the Tempa del Vento and Figliarola faults. In particular, the geometrical features of the two faults are imaged in seismic lines S1 and S2 (Figure 12; see traces of seismic profiles in Figure 2). The two profiles can be interpreted in light of the stratigraphic data provided by the Costa Molina 2 and Tempa del Vento well logs [30] and VIDEPI web site. In both the seismic profiles the faults tend to join downwards while cutting through the tectonic contact separating the Liguride from the Lagonegro Units (Figure 12).

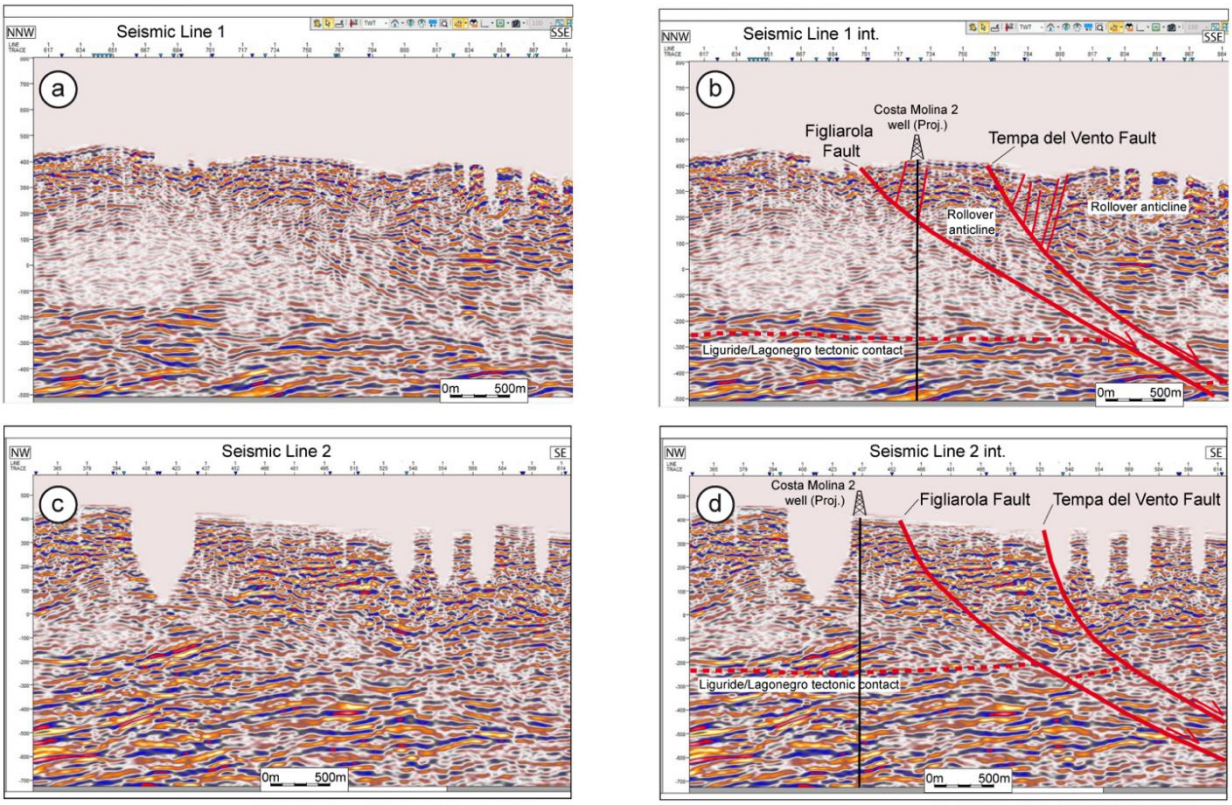

Figure 12. (**a**) Seismic line S1; (**b**) interpretation; (**c**) Seismic line S2; (**d**) interpretation. Interpretations are based on the stratigraphy of the Tempa del Vento and Costa Molina 2 well logs. The Costa Molina 2 well has been projected orthogonally to the seismic sections.

Moreover, line S1 clearly shows a rollover anticline at the hanging wall of the Tempa del Vento and Figliarola faults, which is consistent with a listric geometry of the fault trajectory. It also shows a series of antithetic normal faults affecting the rollover anticline, which likely resulted from crestal collapse [65] during slip along the listric fault. The curved geometry displayed by the two faults at depth is also consistent with a listric geometry, even though velocity effects connected to lithological differences between the Liguride and the Lagonegro Units cannot be excluded. It is important to note that the apparent dip angles of the fault planes decrease from line S2 to line S1, due to the different orientations of the seismic profiles with respect to the strike of the faults. The listric geometry and the tendency of the two structures to join at depth indicates that Figliarola and the Tempa del Vento faults are connected and rooted at a common detachment level.

8. Discussion

The detailed stratigraphic and structural analysis carried out along the southeastern sector of the Agri Valley, with the support of new biostratigraphic data, enabled us to

redefine the geological setting of an important sector of the Agri Valley, where the distinction between different Cenozoic flyschoid units allowed the detection of important tectonic structures. In particular, mapping, correlation and age attribution of different marly intervals allowed us to extend the presence of the Albidona Formation in an area previously ascribed to the Gorgoglione Formation, with the NE-trending Tempa del Vento Fault tectonically separating the two formations. The new findings represent an important update for the available geological maps (sheets 505 and 506 [5,6]) and encourage further discussion about the age of the Albidona Formation. They also provide new evidence for understanding the relationships between tectonics and sedimentation in thrust-sheet top basins, which is crucial for reconstructing the tectonic evolution of the southern Apennines thrust and fold belt. The main implications will be discussed in the next sections.

8.1. Statigraphic Characteristics and Age of the Albidona Formation at the Monte dell'Agresto in Comparison with the Albidona Formation Type-Area

The stratigraphic succession exposed at Monte dell'Agresto share many characteristics with the Albidona Formation succession exposed in the type-area [33]. Lithological and stratigraphical similarities are represented by the common occurrence of a lower portion (member B–C) consisting of alternating sandstone, clay and marly intervals and an upper portion (member D) characterized by alternating coarse-grained sandstones and conglomerates. Another striking similarity is the middle-late Eocene age exhibited by both the study succession and the Albidona type-area succession, according to Baruffini et al. [33]. Nevertheless, regarding the age attribution, some significant discrepancies emerged as well. In fact, while the Barthonian/lower Priabonian age of member D is consistent with the type-area succession, the age of member B–C is different. Very interestingly, the time span encompassed by member B–C at Monte dell'Agresto includes the boundary between the biozones NP15 and NP16 that, in the Albidona type-area is not preserved because of an unconformity producing an important intraformational hiatus at the base of member D. This means that the studied succession shows a less pronounced unconformity between members B–C and D, probably indicating that the Albidona Formation of Monte dell'Agresto was less affected by synsedimentary tectonics and basin instability when compared to the type-area. In conclusion, the member B–C of the Albidona succession exposed at Monte dell'Agresto can be considered in part complementary with that exposed in the type-area.

The Eocene ages obtained in the present study might be useful for discussing the effective age of the Albidona Formation exposed in the Agri Valley area. In fact, it strongly contrasts with the early Miocene age indicated in the official geological maps [5,6]. In our opinion, this latter age attribution is not robustly supported by data. In fact, based on the descriptions accompanying the maps, this age has been inferred by stratigraphic intervals located outside of the mapped areas. In addition, the authors never considered the Agresto succession for age determinations, since it was originally attributed to the Gorgoglione Formation.

The Eocene age is also supported by subsurface data provided by hydrocarbon wells. In particular, the Costa Molina 2 and Costa Molina 3 wells (Figure 2) clearly report the occurrence of Eocene deposits attributable to the Albidona Formation. Moreover, the Tempa del Vento well (Figure 2) shows the occurrence of Eocene deposits right below the Gorgoglione basal unconformity. The Costa Molina 1 well log reports the occurrence of Miocene deposits in the first hundreds of meters. However, more recent stratigraphic reinterpretations carried out by ENI, have questioned this age.

Said that, we cannot exclude that the uppermost portion of the Albidona Formation can be attributed to the lower Miocene, as recently documented in the type-area [46]. However, our data indicate that a large portion of this formation was deposited during the Eocene. A similar age interpretation is provided in the stratigraphic scheme by Vezzani et al. [48], where the Albidona Formation encompasses the Eocene—early Miocene age interval.

8.2. Geodynamic Significance of the Albidona Formation

Clast composition of coarse-grained sediments pertaining to the Albidona Formation provides useful indications about the tectonically active source areas and consequently on the geodynamic scenario at the time of deposition. Obviously, particularly suited at this aim are the coarse-grained sediments represented by conglomerates and the level of pebbly mudstone. The study of these lithologies revealed that most of the clasts derived from a crystalline basement comparable to the uppermost portion of the continental crustal section exposed in the Sila Massif of Calabria [66], where low to medium grade metamorphic rocks are intruded by granodiorites and by later porphyritic dykes [67,68]. On the other hand, the ophiolitic material occurring in the pebbly mudstone, mainly represented by pillow basalts, microgabbro and reddish to greenish cherts, is consistent with the provenance of these clasts from the Liguride accretionary wedge, whose relics are currently exposed in the Pollino area of Basilicata and in Northern Calabria [4,22,69,70]. Therefore, the available data clearly suggest that the Calabrian Arc and the Liguride oceanic palaeodomain were strongly involved by active tectonics in the source area of the Albidona Formation, corresponding to the Liguride accredionary wedge. The search for evidence about a possible involvement in the deformation of the African paleomargin has been fruitless since no pebbles clearly derived from either the Apennine Platform or the Lagonegro Basin have been recognized. Possible sediments sourced from the Apennine Platform might be represented by the marly intervals. However, according to Colella and Zuffa [35], they could just represent very distal sediments supplied by the western margin of the platform located in the foreland setting of the Liguride accretionary wedge. Moreover, very fine grained megaturbidites, such as those generated by tsunami waves, might travel for long distances and transport large amount of carbonate mud, as indicated by Cita et al. ii [38] for the homogenites of the Mediterranean basin. In conclusion, our evidence about clast composition are in good agreement with the geodynamic model proposed by Patacca and Scandone [2] and Vezzani et al. ii [48] which suggests that the Albidona Formation was deposited in a thrust sheet top basin located above the Calabride/Liguride accretionary wedge, during subduction of the oceanic crust of the Ligurian Tethys. Deep subduction followed by fast exhumation of the Tethyan crust during Eocene is documented by radiometric ages and thermobarometry obtained for high-P bluschists from Northern Calabria [71,72].

8.3. Tectonic Setting of the Study Area

Study on fold axes orientations in the investigated area revealed the presence of at least two folding phases showing E-W and NW-SE hinge directions (stereoplot C and D in Figure 8). Occurrence of E-W hinge orientations represent an anomaly for the considered sector of the southern Apennines, where N- to NW-trending structures with an average NE-facing tectonic transport direction have been recognized [73]. This anomaly further supports the results obtained by the study of clast composition namely that the Albidona Formation was deposited in a thrust top basin on the Liguride accretionary wedge that underwent deformation during subduction of the Ligurian Tethys. In fact, the southwards vergence of the D1 folds recognized in the Albidona Formation can be compared with similar structures, showing a tectonic transport toward SW, recognized in the internal Units of the southern Apennines by Vitale and Ciarcia [74]. The same Authors refer the age of this early deformation stage to the early-middle Miocene. Folding stage D2 is related to later evolutionary stages of the southern Apennines thrust belt.

8.4. Significance and Interpretation of the NE-Trending Faults

NE-trending faults occurring in the southern Apennines are largely associated with the Pliocene to Pleistocene evolution of the thrust belt. These tectonic structures generally consist of either right or left—lateral strike slip faults offsetting pre-existing contractional structures, associated with the build-up of the chain, or forming lateral ramps accommodating the thrust emplacement [8,75]. Although predominant, NE-trending strike slip faults are not exclusive in the southern Apennines and an increasing number of NE-trending normal

faults have been recognized. These latter faults have been associated to earlier extensional tectonic stages [76] or to the activation of low—angle normal faults (LANF) [77–79].

The NE-trending Figliarola and the Tempa del Vento faults represent the main extensional structures recognized in the study area. Standing on the geometrical characteristics described in the previous sections, such as the listric geometry observed in the seismic profiles, these structures can be interpreted as SE-dipping intermediate to low angle normal faults. A geological cross-section (Figure 13) allowed assessing the cumulative displacement of the Tempa del Vento and Figliarola faults.

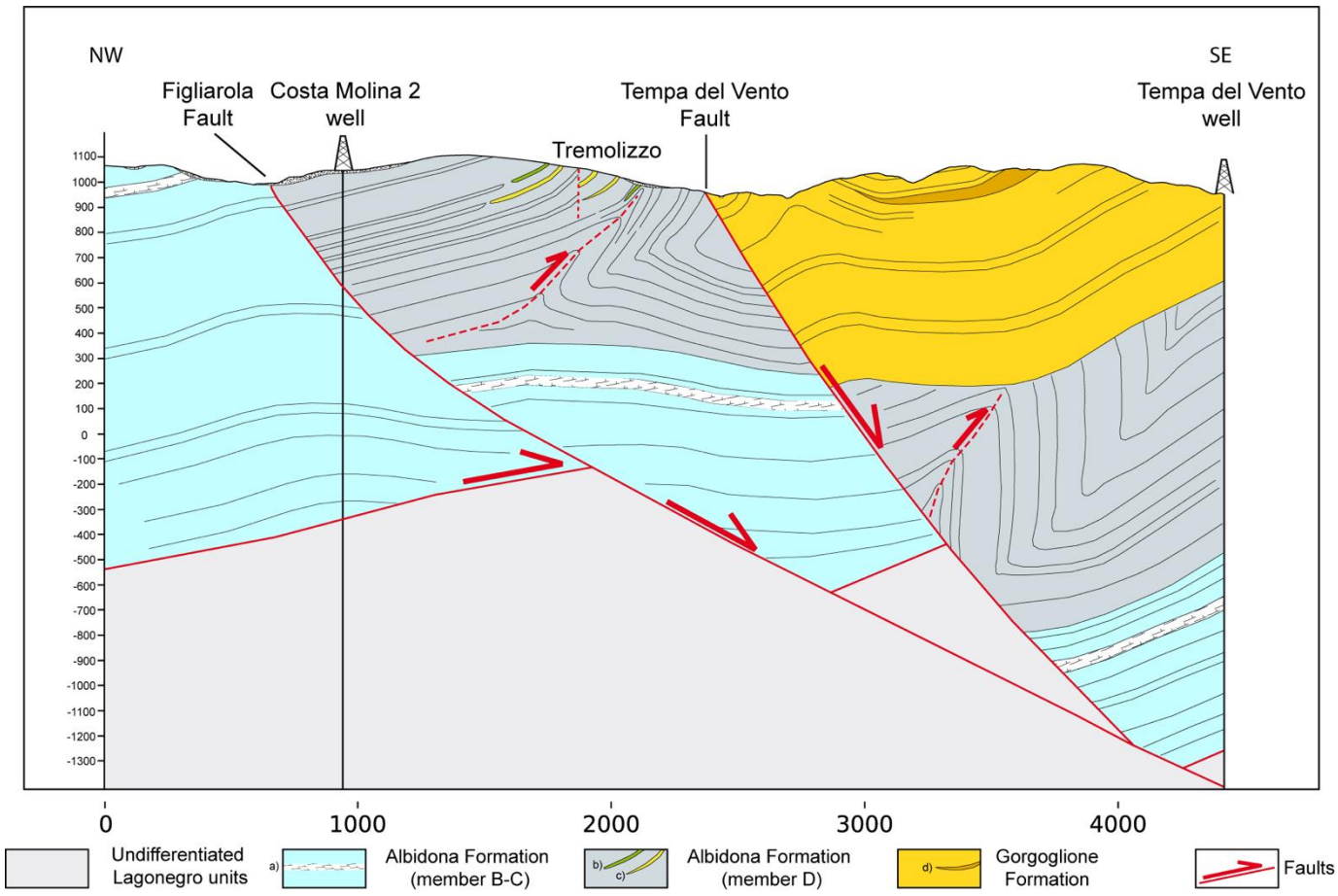

Figure 13. Interpretative cross-section of the M. dell'Agresto—Contrada La Rossa area, showing the overall geometry and displacement of the Figliarola—Tempa del Vento Fault system. Legend: (a) marly marker horizon; (b) microconglomerate; (c) sandstone; (d) conglomerate.

The interpretation presented in the geological cross-section relies on the aforementioned seismic lines and on the data obtained from the Costa Molina 2 and Tempa del Vento wells (Figures 2 and 13). Considering that both normal faults are probably rooted at a common detachment level, the Figliarola Fault can be interpreted as the major structure and the Tempa del Vento Fault as a secondary splay. The cumulative displacement of the two faults can be estimated by considering the marly marker horizon recognized by geological mapping at the footwall of the Figliarola Fault, within the Albidona member B–C, and a similar horizon recognized in the stratigraphic log of the Tempa del Vento well, located at a depth of 1550 m at the hangingwall of the Tempa del Vento Fault. By considering this marker bed, the cumulative displacement of the Figliarola and Tempa del Vento Faults can be estimated at about 1800 m.

8.5. Further Implications

Recognition of the Albidona Formation and previously unknown tectonic structures in the study area has important consequences on reservoir modelling in the Val d'Agri oil field. In particular, based on the present study, it will be possible to update the seismic velocity model, considering the petrophysical characteristics of the Albidona Formation instead of the Gorgoglione Formation. In addition, faults recognized for the first time in the study area will be considered in order to improve the 3D model of the Agri Valley.

The widespread presence of the Albidona Formation in the study area has also strong environmental implications regarding, in particular, the definition of the chemical composition of soils. Knowledge of the composition of soils developed on peculiar rock types is fundamental for differentiating the background concertation of elements connected to either geogenic or anthropogenic processes. In this context, the recognition of the pebbly mudstone interval of the Albidona Formation, containing clasts derived from ophiolitic, igneous and metamorphic source areas, can be helpful in better understanding anomalous concentrations of some elements in soils.

9. Conclusions

The present work stresses on the importance of performing an accurate field mapping for the understanding of surface and subsurface geology. At this aim we presented the case study of the Agri Valley in southern Italy where field survey allowed to revise the distribution of two major Cenozoic turbiditic units of the Southern Apennines (the Albidona and Gorgoglione Formations) and to identify three distinct stratigraphic marker intervals in the Albidona Formation that resulted very useful for stratigraphic correlations both in outcrop and subsurface. From the older to the younger the three intervals are (i) a 40 m thick marly interval, (ii) a pebbly mudstone and (iii) a sandstone interval.

Biostratigraphic analysis performed on the marly level and other similar intervals distributed at different stratigraphic highs in the study succession allowed the attribution of the Albidona Formation to the Eocene. Different facies characteristics and age determinations allowed the differentiation of the Albidona Formation in two members, with the older one, identified as member B–C, Lutetian in Age, consisting of alternating sandstones and clays and the younger one, Barthonian/Priabonian in age, identified as member D, consisting in alternating sandstones and conglomerates.

The geometrical relationships between the two members and with the Miocene Gorgoglione Formation allowed recognising two major NE-trending normal faults, documented for the first time in the study area. These structures, named, respectively, as Figliarola and Tempa del Vento faults, have also been recognized in the subsurface by means available seismic lines provided by ENI.

Recognition of the marker marly horizon in the stratigraphy of Costa Molina and Tempa del Vento wells allowed us to calculate the cumulative displacement of the Figliarola and Tempa del Vento Faults that can be estimated to about 1800 m.

Author Contributions: Conceptualization, G.P. (Giacomo Prosser) and G.P. (Giuseppe Palladino); Data curation, G.P. (Giacomo Prosser), G.P. (Giuseppe Palladino), E.M.B., M.R. and D.E.C.; Formal analysis, G.P. (Giacomo Prosser), G.P. (Giuseppe Palladino), E.M.B., M.R. and D.E.C.; Investigation, G.P. (Giacomo Prosser), G.P. (Giuseppe Palladino), E.M.B., M.R. and D.E.C.; Methodology, G.P. (Giacomo Prosser), E.M.B., M.R. and D.E.C.; Project administration, D.A. and F.C.; Resources, D.A.; Software, G.P. (Giacomo Prosser) and G.P. (Giuseppe Palladino); Supervision, G.P. (Giacomo Prosser), D.A., F.C., M.R. and D.E.C.; Validation, G.P. (Giacomo Prosser), D.A. and F.C.; Visualization, G.P. (Giacomo Prosser), G.P. (Giuseppe Palladino), E.M.B., M.R. and D.E.C.; Writing—original draft, G.P. (Giacomo Prosser), G.P. (Giuseppe Palladino), E.M.B., M.R. and D.E.C.; Writing—review & editing, G.P. (Giacomo Prosser), D.A. and F.C. All authors have read and agreed to the published version of the manuscript.

Funding: This research received no external funding.

Institutional Review Board Statement: Not applicable.

Informed Consent Statement: Not applicable.

Acknowledgments: We very grateful to the editor G. Wang and the guest editors D. Liotta, G. Molli and A. Cipriani for the opportunity to share our research in the Special Issue "The Apennines: Tectonics, Sedimentation, and Magmatism from the Palaeozoic to the Present". We are also grateful to two anonymous referees for their critical reviews that helped improve this paper.

Conflicts of Interest: The authors declare no conflict of interest.

References

1. Prosser, G.; Schiattarella, M.; Tramutoli, M.; Doglioni, C.; Harabaglia, P.; Bigozzi, A. Una sezione rappresentativa dell'Appennino meridionale. In Proceedings of the Conferenza Sulla Ricerca Scientifica in Basilicata, Potenza, Italy, 29 February–1 March 1996.
2. Patacca, E.; Scandone, P. Geology of Southern Apennines. Bollettino della Società Geologica Italiana. *Ital. J. Geosc.* **2007**, *7*, 75–119.
3. Carbone, S.; Catalano, S.; Lazzari, S.; Lentini, F.; Monaco, C. Presentazione della carta geologica del bacino del Fiume. *Agric. Mem. Soc. Geol. Ital.* **1991**, *47*, 129–143.
4. Bonardi, G.; Amore, F.O.; Ciampo, G.; de Capoa, P.; Miconnet, P.; Perrone, V. Il Complesso Liguride Auctorum: Stato delle conoscenze e problemi aperti sulla sua evoluzione pre-appenninca ed i suoi rapporti con l'arco calabro. *Mem. Soc. Geol. Ital.* **1988**, *41*, 17–35.
5. Sevizio Geologico d'Italia, ISPRA, 2014. Carta Geologica d'Italia Alla Scala 1:50,000, Foglio 505 "Moliterno". Available online: https://www.isprambiente.gov.it/Media/carg/505_MOLITERNO/Foglio.html (accessed on 30 December 2020).
6. Sevizio Geologico d'Italia, ISPRA, 2005. Carta Geologica d'Italia Alla Scala 1:50,000, Foglio 506 "Sant'Arcangelo". Available online: https://www.isprambiente.gov.it/Media/carg/506_SANT_ARCANGELO/Foglio.html (accessed on 30 December 2020).
7. Giano, S.I.; Maschio, L.; Alessio, M.; Ferranti, L.; Improta, S.; Schiattarella, M. Radiocarbon dating of active faulting in the Agri high valley, southern Italy. *J. Geodyn.* **2000**, *29*, 371–386. [CrossRef]
8. Cello, G.; Gambini, R.; Mazzoli, S.; Read, A.; Tondi, E.; Zucconi, V. Fault zone characteristics and scaling properties of the Val d'Agri Fault System (Southern Apennines, Italy). *J. Geodyn.* **2000**, *29*, 293–307. [CrossRef]
9. Hippolyte, J.-C.; Angelier, J.; Roure, F. A major geodynamic change revealed by Quaternary stress patterns in the southern Apennines (Italy). *Tectonophysics* **1994**, *230*, 199–210. [CrossRef]
10. Ferranti, L.; Oldow, J.S. Latest Miocene to Quaternary horizontal and vertical displacement rates during simultaneous contraction and extension in the Southern Apennines orogen, Italy. *Terra Nova* **2005**, *17*, 209–214. [CrossRef]
11. Malinverno, A.; Ryan, W.B.F. Extension in the Tyrrhenian Sea and shortening in the Apennines as result of arc migration driven by sinking of the lithosphere. *Tectonics* **1986**, *5*, 227–245. [CrossRef]
12. Royden, L.; Patacca, E.; Scandone, P. Segmentation and configuration of subducted lithosphere in Italy: An important control on thrust-belt and foredeep-basin evolution. *Geology* **1987**, *15*, 714–717. [CrossRef]
13. Patacca, E.; Sartori, R.; Scandone, P. Tyrrhenian basin and Apenninic arcs: Kinematic relations since Late Tortonian times. *Mem. Soc. Geol. Ital.* **1990**, *45*, 425–451.
14. Doglioni, C. A proposal for the kinematic modelling of W-dipping subductions—Possible applications to the Tyrrhenian-Apennines system. *Terra Nova* **1991**, *3*, 423–434. [CrossRef]
15. Morandi, S.; Ceragoli, E. Integrated interpretation of seismic and resistivity images across the «Val d'Agri» graben (Italy). *Ann. Geophys.* **2002**, *45*, 259–271.
16. Maschio, L.; Ferranti, L.; Burrato, P. Active extension in Val d'Agri area, Southern Apennines, Italy: Implications for the geometry of the seismogenic belt. *Geophys. J. Int.* **2005**, *162*, 591–609. [CrossRef]
17. Burrato, P.; Valensise, G. Rise and Fall of a Hypothesized Seismic Gap: Source Complexity in the Mw 7.0 16 December 1857 Southern Italy Earthquake. *Bull. Seism. Soc. Am.* **2008**, *98*, 139–148. [CrossRef]
18. Improta, L.; Ferranti, L.; De Martini, P.M.; Piscitelli, S.; Bruno, P.P.; Burrato, P.; Civico, R.; Giocoli, A.; Iorio, M.; D'Addezio, G.; et al. Detecting young, slow-slipping active faults by geologic and multidisciplinary high-resolution geophysical investigations: A case study from the Apennine seismic belt, Italy. *J. Geophys. Res. Space Phys.* **2010**, *115*, 11307. [CrossRef]
19. Shiner, P.; Beccacini, A.; Mazzoli, S. Thin-skinned versus thick-skinned structural models for Apulian carbonate reservoirs: Constraints from the Val d'Agri Fields, S Apennines, Italy. *Mar. Pet. Geol.* **2004**, *21*, 805–827. [CrossRef]
20. Handy, M.R.; Schmid, S.M.; Bousquet, R.; Kissling, E.; Bernoulli, D. Reconciling plate-tectonic reconstructions of Alpine Tethys with the geological–geophysical record of spreading and subduction in the Alps. *Earth-Sci. Rev.* **2010**, *102*, 121–158. [CrossRef]
21. Knott, S.D. The Liguride Complex of Southern Italy—A Cretaceous to Paleogene accretionary wedge. *Tectonophysics* **1987**, *142*, 217–226. [CrossRef]
22. Vitale, S.; Ciarcia, S.; Fedele, L.; Tramparulo, F.D. The Ligurian oceanic successions in southern Italy: The key to decrypting the first orogenic stages of the southern Apennines-Calabria chain system. *Tectonophysics* **2019**, *750*, 243–261. [CrossRef]
23. Scandone, P. Studi di geologia lucana: Carta dei terreni della serie calcareo-silico-marnosa e note illustrative. *Boll. Soc. Natur. Napoli* **1972**, *273*, 225–299.
24. Bucci, F.; Novellino, R.; Tavarnelli, E.; Prosser, G.; Guzzetti, G.; Cardinali, M.; Gueguen, E.; Guglielmi, P.; Adurno, I. Frontal collapse during thrust propagation in mountain belts: A case study in the Lucanian Apennines, Southern Italy. *J. Geol. Soc.* **2014**, *171*, 571–581. [CrossRef]

25. Patacca, E.; Scandone, P. Late thrust propagation and sedimentary response in the thrust-beltforedeep system of the Southern Apennines (Pliocene-Pleistocene). In *Anatomy of an Orogen: The Apennines and Adjacent Mediterranean Basins*; Vai, G.B., Martini, I.P., Eds.; Kluwer Academic Publishers: London, UK, 2001.
26. Noguera, A.; Rea, G. Deep structure of the Campanian–Lucanian Arc (Southern Apennine, Italy). *Tectonophysics* **2000**, *324*, 239–265. [CrossRef]
27. Boiano, U. Anatomy of a siliciclastic turbidite basin: The Gorgoglione Flysch, Upper Miocene, southern Italy: Physical stratigraphy, sedimentology and sequence-stratigraphic framework. *Sediment. Geol.* **1997**, *107*, 231–262. [CrossRef]
28. Cavalcante, F.; Fiore, S.; Lettino, A.; Piccarreta, G.; Tateo, F. Illite-smectite mixed layers in Sicilide shales and piggy-back deposits of the Gorgoglione Formation (Southern Apennines): Geological inference. *Boll. Soc. Geol. Ital.* **2007**, *126*, 241–254.
29. Cavalcante, F.; Prosser, G.; Agosta, F.; Belviso, C.; Corrado, G. Post-depositional history of the Miocene Gorgoglione Formation (southern Apennines, Italy): Inferences from mineralogical and structural analyses. *Bull. Soc. Géol. Fr.* **2015**, *186*, 243–256. [CrossRef]
30. Buttinelli, M.; Improta, L.; Bagh, S.; Chiarabba, C. Inversion of inherited thrusts by wastewater injection induced seismicity at the Val d'Agri oilfield (Italy). *Sci. Rep.* **2016**, *6*, 37165. [CrossRef]
31. Selli, R. Il Paleogene nel quadro della geologia dell'Italia centro-meridionale. *Mem. Soc. Geol. Ital.* **1962**, *3*, 737–789.
32. Zuppetta, A.; Russo, M.; Turco, E.; Gallo, L. Età e significato della Formazione di Albidona in Appennino Meridionale. *Boll. Soc. Geol. Ital.* **1984**, *103*, 159–170.
33. Baruffini, L.; Lottaroli, F.; Torricelli, S.; Lazzari, D. Stratigraphic revision of the Eocene Albidona Formation in the type locality (Calabria, southern Italy). *Riv. Ital. Paleontol. Stratigr.* **2000**, *106*, 73–98.
34. Critelli, S.; Muto, F.; Tripodi, V.; Perri, F. Link between thrust tectonics and sedimentation processes of stratigraphic sequences from the southern Apennines foreland basin system, Italy. *Rend. Online Soc. Geol. Ital.* **2013**, *25*, 21–42.
35. Colella, A.; Zuffa, G.G. Megastrati carbonatici e silicoclastici della Formazione di Albidona (Miocene, Appennino meridionale): Implicazioni paleogeografiche. *Mem. Soc. Geol. Ital.* **1988**, *41*, 791–807.
36. Dietrich, D.; Scandone, P. The position of basic and ultrabasic rocks in the tectonic units of the southern Apennines. *Atti dell'Accademia Pontiana* **1972**, *21*, 1–15.
37. Kastens, K.A.; Cita, M.B. Tsunami-induced sediment transport in the abyssal Mediterranean Sea. *GSA Bull.* **1981**, *92*, 845–857. [CrossRef]
38. Cita, M.B.; Camerlenghi, A.; Rimoldi, B. Deep-sea tsunami deposits in the eastern Mediterranean: New evidence and depositional models. *Sediment. Geol.* **1996**, *104*, 155–173. [CrossRef]
39. Pavan, G.; Pirini, C. Microfossili cretacici ed eocenici nella zona di Monte Falapato (Lucania). *Mem. Soc. Geol. Ital.* **1963**, *4*, 1105–1134.
40. Mostardini, F.; Pieri, M.; Pirini, C. Stratigrafia del foglio 212, Montalbano Jonico. *Boll. Serv. Geol. Ital.* **1966**, *87*, 541–547.
41. Ogniben, L. Schema introduttivo alla geologia del confine calabro-lucano. *Mem. Soc. Geol. Ital.* **1969**, *8*, 453–763.
42. Vezzani, L. Nota preliminare sulla stratigrafia della Formazione di Albidona. *Boll. Soc. Geol. Ital.* **1966**, *85*, 767–776.
43. Vezzani, L. Distribuzione, facies e stratigrafia della Formazione del Saraceno (Albiano—Daniano) nell'area compresa tra il Mare Jonio e il Torrente Frido. *Geol. Rom.* **1968**, *7*, 229–276.
44. Vezzani, L. Il Flysch di Albidona nell'area del confine tra Calabria e Lucania. *Geol. Rom.* **1970**, *9*, 101–126.
45. Bonardi, G.; Ciampo, G.; Perrone, V. La Formazione di Albidona nell'Appennino calabro-lucano: Ulteriori dati stratigrafici e relazioni con le unità esterne appenniniche. *Boll. Soc. Geol. Ital.* **1985**, *104*, 539–549.
46. Sevizio Geologico d'Italia, ISPRA, 2009. Carta Geologica d'Italia alla scala 1:50,000, Foglio 535 "Trebisacce". Available online: https://www.isprambiente.gov.it/Media/carg/535_TREBISACCE/Foglio.html (accessed on 30 December 2020).
47. Lentini, F.; Carbone, S.; Catalano, S.; Monaco, C. Confronti sedimentologico petrografici e posizione strutturale del Flysch di Albidona e di Gorgoglione nella media Val d'Agri (Appennino lucano). *Mem. Soc. Geol. Ital.* **1987**, *38*, 259–263.
48. Vezzani, L.; Festa, A.; Ghisetti, F.C. *Geology and Tectonic Evolution of the Central-Southern Apennines, Italy*; Geological Society of America: Boulder, CO, USA, 2010.
49. Patacca, E.; Scandone, P.; Bellatalla, M.; Perilli, N.; Santini, U. Numidian sand event in the Southern Apennines. *Mem. Soc. Geol. Padova* **1992**, *43*, 297–337.
50. Palladino, G.; Parente, M.; Prosser, G.; Di Staso, A. Tectonic control on the deposition of the Lower Miocene sediments of the Monti della Maddalena ridge (Southern Apennines): Synsedimentary extensional deformation in a foreland setting. *Boll. Soc. Geol. Ital.* **2008**, *127*, 317–335.
51. Okada, H.; Bukry, D. Supplementary modification and introduction of code numbers to the low-latitude coccolith biostratigraphic zonation (Bukry, 1973; 1975). *Mar. Micropaleontol.* **1980**, *5*, 321–325. [CrossRef]
52. Martini, E. Standard Tertiary and Quaternary calcareous nannoplankton zonation. In *Proceedings of the Second Planktonic Conference, Roma, 1970*; Tecnoscienza: Roma, Italy, 1971; pp. 739–765.
53. Perch-Nielsen, K. Cenozoic calcareous nannofossils. In *Plankton Stratigraphy*; Bolli, H.M., Saunders, J.B., PerchNielsen, K., Eds.; Cambridge University Press: Cambridge, UK, 1985; pp. 427–554.
54. Bown, P.R. *Calcareous Nannofossil Biostratigraphy*; Kluwer Academic Publishers: Norwell, MA, USA, 1998; pp. 1–315.
55. Gradstein, F.M.; Ogg, J.G.; Schmitz, M.D.; Ogg, G.M. *The Geological Time Scale 2012*; Elsevier: Amsterdam, The Netherlands, 2012.
56. Priest, S.D. *Discontinuity Analysis for Rock Engineering*; Springer Science and Business Media LLC.: Secaucus, NJ, USA, 1993.

57. Ortega, O.J.; Marrett, R.A.; Laubach, S.E. A scale-independent approach to fracture intensity and average spacing measurement. *AAPG Bull.* **2006**, *90*, 193–208. [CrossRef]
58. Bouma, A.H. *Sedimentology of Some Flysch Deposits*; Elsevier: Amsterdam, The Netherlands, 1962.
59. Sartoni, S.; Crescenti, U. *Ricerche Biostratigrafiche nel Mesozoico dell'Appennino Meridionale*; Museo Geologico Giovanni Capellini: Bologna, Italy, 1962; Volume 29, pp. 153–302.
60. Scandone, P.; Sgrosso, I. Flysch con Inocerami nella Valle del Cavolo presso Tramutola (Lucania). *Boll. Soc. Natur. Napoli* **1964**, *73*, 166–175.
61. Giannandrea, P.; LoIacono, F.; Maiorano, P.; Lirer, F.; Puglisi, D. Geological map of the eastern sector of the Gorgoglione Basin (southern Italy). *Ital. J. Geosci.* **2016**, *135*, 120–141. [CrossRef]
62. Ramsay, J.G. *Folding and Fracturing of Rocks*; McGraw-Hill: New York, NY, USA, 1967.
63. Kim, Y.-S.; Peacock, D.C.; Sanderson, D.J. Fault damage zones. *J. Struct. Geol.* **2004**, *26*, 503–517. [CrossRef]
64. Choi, J.-H.; Edwards, P.; Ko, K.; Kim, Y.-S. Definition and classification of fault damage zones: A review and a new methodological approach. *Earth-Sci. Rev.* **2016**, *152*, 70–87. [CrossRef]
65. McClay, K. Extensional fault systems in sedimentary basins: A review of analogue model studies. *Mar. Pet. Geol.* **1990**, *7*, 206–233. [CrossRef]
66. Caggianelli, A.; Prosser, G. An exposed cross-section of Late Hercynian upper and intermediate continental crust exposed in the Sila Nappe (Calabria, Southern Italy). *Period. Mineral.* **2001**, *70*, 275–301.
67. Langone, A.; Godard, G.; Prosser, G.; Caggianelli, A.; Rottura, A.; Tiepolo, M. P–T–t path of the Hercynian low-pressure rocks from the Mandatoriccio complex (Sila Massif, Calabria, Italy): New insights for crustal evolution. *J. Metamorph. Geol.* **2010**, *28*, 137–162. [CrossRef]
68. Festa, V.; Langone, A.; Caggianelli, A.; Rottura, A. Dike magmatism in the Sila Grande (Calabria, southern Italy): Evidence of Pennsylvanian–Early Permian exhumation. *Geosophy* **2010**, *6*, 549–566. [CrossRef]
69. Cavalcante, F.; Belviso, C.; Finizio, F.; Lettino, A.; Fiore, S. *Carta Geologica delle Unità Liguridi Dell'area del Pollino (Basilicata): Nuovi dati Geologici, Mineralogici e Petrografici*; Digilabs: Bari, Italy, 2009.
70. Liberi, F.; Morten, L.; Piluso, E. Geodynamic significance of ophiolites within the Calabrian Arc. *Isl. Arc* **2006**, *15*, 26–43. [CrossRef]
71. Shimabukuro, D.H.; Wakabayashi, J.; Alvarez, W.; Chang, S.-C. Cold and old: The rock record of subduction initiation beneath a continental margin, Calabria, southern Italy. *Lithosphere* **2012**, *4*, 524–532. [CrossRef]
72. Tursi, F.; Bianco, C.; Brogi, A.; Caggianelli, A.; Prosser, G.; Ruggieri, G.; Braschi, E. Cold subduction zone in northern Calabria (Italy) revealed by lawsonite–clinopyroxene blueschists. *J. Metamorph. Geol.* **2020**, *38*, 451–469. [CrossRef]
73. Mazzoli, S.; Barkham, S.; Cello, G.; Gambini, R.; Mattioni, L.; Shiner, P.; Tondi, E. Reconstruction of continental margin architecture deformed by the contraction of the Lagonegro Basin, southern Apennines, Italy. *J. Geol. Soc.* **2001**, *158*, 309–319. [CrossRef]
74. Vitale, S.; Ciarcia, S. Tectono-stratigraphic and kinematic evolution of the southern Apennines/Calabria–Peloritani Terrane system (Italy). *Tectonophysics* **2013**, *583*, 164–182. [CrossRef]
75. Bonini, M.; Sani, F. Pliocene-Quaternary transpressional evolution of the Anzi-Calvello and Northern S. Arcangelo basins (Basilicata, Southern Apennines, Italy) as a consequence of deep-seated fault reactivation. *Mar. Pet. Geol.* **2000**, *17*, 909–927. [CrossRef]
76. Bucci, F.; Novellino, R.; Guglielmi, P.; Prosser, G.; Tavarnelli, E. Geological map of the northeastern sector of the high Agri Valley, Southern Apennines (Basilicata, Italy). *J. Maps* **2012**, *8*, 282–292. [CrossRef]
77. Ferranti, L.; Oldow, J.S.; Sacchi, M. Pre-Quaternary orogen-parallel extension in the Southern Apennine belt, Italy. *Tectonophysics* **1996**, *260*, 325–347. [CrossRef]
78. Novellino, R.; Prosser, G.; Spiess, R.; Viti, C.; Agosta, F.; Tavarnelli, E.; Bucci, F. Dynamic weakening along incipient low-angle normal faults in pelagic limestones (Southern Apennines, Italy). *J. Geol. Soc.* **2015**, *172*, 283–286. [CrossRef]
79. Giano, S.I.; Pescatore, E.; Agosta, F.; Prosser, G. Geomorphic evidence of Quaternary tectonics within an underlap fault zone of southern Apennines, Italy. *Geomorphology* **2018**, *303*, 172–190. [CrossRef]